



YAŞAR UNIVERSITY
GRADUATE SCHOOL OF NATURAL AND APPLIED SCIENCES

MASTER THESIS

**NOISE ANALYSIS OF AUTOMOTIVE BRAKE
SYSTEMS**

ZEYNEP ERTEKIN

THESIS ADVISOR: DR. NALAN ÖZKURT

ELECTRICAL AND ELECTRONICS ENGINEERING

PRESENTATION DATE: 22.05.2018

BORNOVA / İZMİR
MAY 2018

We certify that, as the jury, we have read this thesis and that in our opinion it is fully adequate, in scope and in quality, as a thesis for the degree of Master of Science.

Jury Members:

Asst. Prof. Dr. Nalan ÖZKURT
Yaşar University

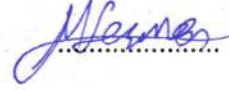
Signature:



Asst. Prof. Dr. Erkan Zeki ENGİN
Ege University



Assoc. Prof. Dr. Mustafa SEÇMEN
Yaşar University



Prof. Dr. Cüneyt GÜZELİŞ
Director of the Graduate School

ABSTRACT

NOISE ANALYSIS OF AUTOMOTIVE BRAKE SYSTEMS

Ertekin, Zeynep

MSc, Electrical Electronics Engineering

Advisor: Asst. Prof. Dr. Nalan Özkurt

May 2018

In this thesis, air disc brakes are investigated in terms of noise using signal processing tools. Inspired by the literature view, sound and vibration data are used in order to detect faults, moreover; many algorithms are proposed to classify the type of the dysfunction. Sounds recorded from a noiseless, a less noisy and a noisy brake by a data acquisition board, are analyzed in time domain, in frequency domain and in time-frequency domain, respectively.

The mean, variance, number of zero crossings, maximum, minimum, and entropy of time windows are calculated and the brakes are classified as noisy and less noisy using k nearest neighbor classification algorithm. The same procedure is repeated for frequency domain considering features mean, variance, spectral roll-off, maximum and entropy. Since time-frequency domain analysis will reveal the characteristics of the sound signals better, qualitative and quantitative analysis has been accomplished by using continuous and discrete wavelet transform. It has been shown that the discrimination between the noisy and less noisy brakes signals can be observed in time-frequency domain clearly.

Key Words: Disc brake systems, noise, wavelet transform, frequency domain, k nearest neighbor (k-NN algorithm)

ÖZ

OTOMOBİL FREN SİSTEMLERİNDE SES ANALİZİ

Ertekin, Zeynep

Yüksek Lisans Tezi, Elektrik Elektronik Mühendisliği

Danışman: Dr. Nalan Özkurt

Mayıs 2018

Bu çalışmada hava diskli frenler, sinyal işleme araçları kullanılarak gürültü açısından incelenmiştir. Literatür taramasından esinlenerek, hataları tespit etmek için ses ve titreşim verileri kullanılmış; hata tipini sınıflandırmak için birçok algoritma önerilmiştir. Bir veri toplama kartı ile gürültüsüz, daha az gürültülü ve gürültülü bir frenden kaydedilen sesler, zaman alanında, frekans alanında ve zaman-frekans alanlarında sırasıyla analiz edilmiştir.

Ortalama, varyans, sıfır geçiş sayısı, en büyük, en küçük ve entropi değerleri zaman penceresinde hesaplanmış ve en yakın komşu algoritması kullanılarak frenler sesli (gürültülü) ve az sesli olarak sınıflandırılmıştır. Aynı prosedür, ortalama, varyans, spektral yuvarlama, en büyük ve entropi gibi frekans öznitelikleri için tekrarlanmıştır. Zaman-frekans ortamı analizi, ses sinyallerinin özelliklerini daha iyi ortaya çıkaracağından, sürekli ve ayrık dalgacık dönüşümü kullanılarak nitel ve nicel analizler gerçekleştirilmiştir. Gürültülü ve daha az gürültülü fren sinyalleri arasındaki ayrımın, zaman-frekans alanında açıkça görülebileceği gösterilmiştir.

Anahtar Kelimeler: Disk fren sistemleri, gürültü, dalgacık, frekans bölgesi, k-en yakın komşuluk

ACKNOWLEDGEMENTS

I would first like to thank my thesis advisor Dr. Nalan Özkurt for her guidance and infinite patience during this study. The door of Dr. Özkurt's office U-114 was always open to me whenever I ran into a trouble spot or had an inquiry about my investigation or typing. She profoundly led me to make this paper to be my own work and guided me in the right way whenever she saw I needed it and became my troubleshooter. All her contributions, time, views and guidance motivated me more which in the end made this study meaningful and enlightening. The eagerness and joy she has for searching and learning was definitely contagious and encouraged me more when I felt lack...

I want to express my frank gratitude to Ege Fren Family for sharing their data, for their considerate approach and supportive manners to a stranger like me at the time.

I earned the friendship of one of my beloved classmates, which I missed when I was a sophomore, Tutku. This study also taught me to change my perspective and not to be biased against people.

I would also like to thank my dearest friend Research Assistant Çağla Sarvan, who constantly backed me up during most of my troubleshootings.

During my M.Sc., from the beginning to the end, I looked for a job in various cities for different positions. My lecturers Dr. Mustafa Seçmen, Dr. Hacer Şekerci, my supervisor Dr. Nalan Özkurt, my friends and family who gave me moral support during those desperate days and encouraged me will be appreciated forever. I learnt the importance of consistency and how to deal with mental breakdown at those times. Thanks to Dr. Özkurt again, I started my first job and had my first official experience.

I would like to verbalize my grateful love to my parents, grandparents and my aunt, who always stand behind me in a caring and supportive way in my life.

Zeynep Ertekin

İzmir, 2018

TEXT OF OATH

I declare and honestly confirm that my study, titled “NOISE ANALYSIS OF AUTOMOTIVE BRAKE SYSTEMS” and presented as a Master’s Thesis, has been written without applying to any assistance inconsistent with scientific ethics and traditions. I declare, to the best of my knowledge and belief, that all content and ideas drawn directly or indirectly from external sources are indicated in the text and listed in the list of references.

Zeynep Ertekin

Signature



May 22, 2018



TABLE OF CONTENTS

ABSTRACT	v
ÖZ	vii
ACKNOWLEDGEMENTS	viii
TEXT OF OATH	ix
TABLE OF CONTENTS	xi
LIST OF FIGURES	xiii
LIST OF TABLES	xv
SYMBOLS AND ABBREVIATIONS	xvii
CHAPTER 1 INTRODUCTION	1
1.1. Description of the Problem	1
1.2. Aim of Research	1
1.3. Literature Review	2
1.4. Brake Systems	5
1.5. Outline of thesis	7
CHAPTER 2 TIME, FREQUENCY AND TIME-FREQUENCY TECHNIQUES	8
2.1. Fourier Series and Fourier Transform	8
2.1.1. Disadvantages of Fourier Transform	10
2.1.2. Short Time Fourier Transform	11
2.2. Wavelet Analysis	15
2.2.1. Requirements for The Wavelet	16
2.2.2. Energy Spectrum of The Wavelet	16
2.2.3. The Wavelet Transform	17
2.2.4. Inverse Wavelet Transform	20
2.2.5. Power Spectra Based Wavelet Energy	22
2.2.6. Scalogram	22
2.2.7. Complex Wavelet	23
2.2.8. Morlet Decomposition of a Signal	26
2.3. Discrete Wavelet Transform	27
2.4. Wavelet Ridges	30
2.5. Fourier Transform vs Short Time Fourier Transform vs Wavelet Transform	33

CHAPTER 3 SOUND ACQUISITION AND PROCESSING.....	35
3.1. Data Acquisition	36
3.2. Time Domain Analysis And Features.....	37
3.2.1. Mean	38
3.2.2. Maximum.....	39
3.2.3. Minimum	40
3.2.4. Variance.....	41
3.2.5. Number of Zero Crossings.....	43
3.2.6. Entropy.....	44
3.2.7. Classification Using Time Domain Features	46
3.3. Frequency Domain Analysis And Features	48
3.3.1. Mean	48
3.3.2. Variance.....	49
3.3.3. Maximum.....	51
3.3.4. Spectral Roll-Off.....	52
3.3.5. Entropy.....	54
3.3.6. Classification Using Frequency Domain Features.....	55
3.4. Time-Frequency Domain Analysis Using Complex Wavelet.....	56
3.5. Time-Frequency Domain Analysis Using Discrete Wavelet	65
CHAPTER 4 CONCLUSIONS AND FUTURE RESEARCH.....	68
REFERENCES	71

LIST OF FIGURES

Figure 1.1. Air Disc Brake.....	7
Figure 2.1. From time domain to frequency domain.....	10
Figure 2.2. Representation of a nonstationary signal, in time and frequency domains.....	11
Figure 2.3. Sliding window function in frequency domain.....	12
Figure 2.4. STFT application.....	12
Figure 2.5. STFT window sizes representation.....	13
Figure 2.6. Wavelet application.....	14
Figure 2.7. Four common wavelets.....	15
Figure 2.8. Dilation and translation of a wavelet	18
Figure 2.9. Schematic representation of the wavelet transform in its time and frequency representations.....	20
Figure 2.10. The signal and the plot of its transformation.....	21
Figure 2.11. Filtering of the embodied signal by wavelet.....	21
Figure 2.12. Morlet Wavelet.....	23
Figure 2.13. Morlet Wavelet and energy spectrum.....	24
Figure 2.14. An analysis of a two component sinusoidal waveform, by Morlet Wavelet.....	25
Figure 2.15. Original Signal and its Morlet Wavelet Transformation.....	26
Figure 2.16. Daubechies wavelets.....	28
Figure 2.17. Filtering of the signal.....	29
Figure 2.18. Shows the comparison between FT, STFT and Wavelet Transform.....	34
Figure 3.1. The imc CRONOSflex 4 channel data acquisition board.....	37
Figure 3.2. Two seconds braking interval representations of less noisy and noisy brake in time domain.....	37
Figure 3.3. The mean of each braking interval in time domain for noisy brake.....	38
Figure 3.4. The mean of each braking interval in time domain for less noisy brake.....	38
Figure 3.5. The maximum of each braking interval in time domain for less noisy brake.....	39
Figure 3.6. The maximum of each braking interval in time domain for noisy brake.....	40
Figure 3.7. The minimum of each braking interval in time domain for less noisy brake.....	40
Figure 3.8. The minimum of each braking interval in time domain for noisy brake.....	41
Figure 3.9. The variance of each braking interval in time domain for less noisy brake.....	42
Figure 3.10. The variance of each braking interval in time domain for noisy brake.....	42
Figure 3.11. The variance of each braking interval in time domain for less noisy brake.....	43

Figure 3.12. The variance of each braking interval in time domain for noisy brake.....	44
Figure 3.13. The entropy of each braking interval in time domain for less noisy brake.....	45
Figure 3.14. The entropy of each braking interval in time domain for noisy brake.....	45
Figure 3.15. Accuracy of classification using time domain features.....	48
Figure 3.16. Two seconds braking interval representations of less noisy and noisy brake in frequency domain.....	48
Figure 3.17. The mean of each braking interval in frequency domain for noisy brake.....	49
Figure 3.18. The mean of each braking interval in frequency domain for less noisy brake.....	49
Figure 3.19. The mean of each braking interval in frequency domain for noisy brake.....	50
Figure 3.20. The mean of each braking interval in frequency domain for less noisy brake.....	50
Figure 3.21. The entropy of each braking interval in time domain for less noisy brake.....	51
Figure 3.22. The entropy of each braking interval in time domain for noisy brake.....	52
Figure 3.23. The spectral roll-of of each braking interval in time domain for noisy brake.....	53
Figure 3.24. The spectral roll-of of each braking interval in time domain for less noisy brake.....	53
Figure 3.25. Average entropies of noisy brake signals in frequency domain.....	54
Figure 3.26. Average entropies of less noisy brake signals in time domain.....	54
Figure 3.27. Spectral roll-off, maximum, variance, mean and entropy features classification accuracy in frequency domain.....	55
Figure 3.28. Comparison of entropy of wavelet ridge images for less noisy and noisy brakes.....	57
Figure 3.29. Time domain, frequency domain and time-frequency domain representations of a noiseless brake, using cmor 1-20 wavelet.....	59
Figure 3.30. Time domain, frequency domain and time-frequency domain representations of less noisy brake, using cmor 1-20 wavelet.....	60
Figure 3.31. Time domain, frequency domain and time-frequency domain representations of a noisy brake, using cmor 1-20 wavelet.....	61
Figure 3.32. Time domain, frequency domain and time-frequency domain representations of a noiseless brake, using cmor 1-10 wavelet.....	62
Figure 3.33. Time domain, frequency domain and time-frequency domain representations of a less noisy brake, using cmor 1-10 wavelet.....	63

Figure 3.34. Time domain, frequency domain and time-frequency domain representations of a noisy brake, using cmor 1-10 wavelet.....64

Figure 3.35. Process of brake classification using DWT.....65

Figure 3.36. Classification accuracy for different order of Daubechies wavelet family66



LIST OF TABLES

Table 3.1. Average of features in time domain for less noisy and noisy brake.....47

Table 3.2. Average of features in frequency domain for less noisy and noisy brake.....55



SYMBOLS AND ABBREVIATIONS

ABBREVIATIONS:

FT	Fourier Transform
FS	Fourier Series
STFT	Short Time Fourier Transform
FFT	Fast Fourier Transform
IFT	Inverse Fourier Transform
WT	Wavelet Transform
DWT	Discrete Wavelet Transform
K-NN	K Nearest Neighbor Algorithm
DTC	Decision Tree Classifier
CR	Current Ripples electric parking brakes (EPB)
EPB	Electronic Parking Brakes
SVM	Support Vector Machine
ANFIS	Adaptive Neuro-Fuzzy Inference System
ABS	Antilock Brake System
MHW	Mexican Hat Wavelet
SVD	Singular Value Decomposition
FWT	Fast Wavelet Transform
Db	Daubechies

CHAPTER 1

INTRODUCTION

1.1. Description of the Problem

In mechanical systems, unexpected noise or vibration might occur eventually due to friction or other physical faults. These symptoms can be seen separately or together. Noise and vibration data have been analyzed frequently in automotive industry in order to increase customer satisfaction. Investigation of noise and vibration data in multicomponent systems requires a clear data acquisition process and a profound examination. In this thesis, two types of faulty brakes which have been reported by drivers to manufacturers with noisy label have been investigated using signal processing tools in order to prove the physical fault.

1.2. Aim of the Research

The aim of this research is to conduct a detailed investigation of brake noises. Most of the brake noises are produced due to the friction of components in the brake. However since the friction phenomenon keeps its unclear mechanism, unwanted sounds from brakes are hard to explain and analyze.

Globally, in automotive industry, faults in brakes are highly important since they assure safety. Due to the fact that, any problem in brakes are investigated deeply until satisfying answers are obtained. By the perspective of consumers, this concludes as an absence of their vehicle during the examination, by the perspective of manufacturers, this refers to work labor and time. Right in this point, automatic and semi-automatic fault detection systems importance can be seen. An innovative approach, investigation of brake noises without dismounting the brake has been performed in this thesis.

Time domain and frequency domain and time-frequency domain analysis for noisy brakes have been carried out, respectively. It has been concluded that analyzing sound and or vibration data in order to classify brakes with respect to noises could be a novel approach. Features such as mean, variance, spectral centroid, spectral roll-off, number of zero crossings, maximum, minimum, and entropy have been investigated to classify less noisy and noisy brakes. Since time-frequency domain analysis will show the characteristics of the sound signals better, qualitative and quantitative analysis has been accomplished using continuous and discrete wavelet transform.

The results are promising that, some qualitative and quantitative features can be used in order to determine brake faults. In the near future, it's been foreseen that, noise and vibration data fed devices will be used to classify disorders not only for brakes but also for other multicomponent systems.

1.3. Literature Review

Brake system is undoubtedly one of the most important control mechanisms in an automobile. A properly working brake system should provide the vehicle to rest in an appropriate time.

Brakes Can Be Classified Considering Their “Working” Mechanisms As Frictional, Pumping Or Electromagnetically Acting Systems. Sometimes One Brake System May Use A Combination Of Above Mentioned Mechanisms. In Order To Slow Or Stop A Moving Vehicle, It Should Be Mechanically, Hydraulically, Pneumatically Or Electromagnetically Forced. In A Near Future, The Conventional Hydraulic Brake Systems Will Replaced By Electrically Operated Brakes Also Called “Brake-By-Wire” (Hwang, 2012).

There are moving components in a brake system and eventually they may wear off due to friction. Therefore, effectiveness and safety of the brake system become unreliable. The disorders of a brake system can be understood following some symptoms or warning indicators such as odor of brake lining, vibrations, noise and monitoring digital images on the car. The engineering problem focused on this thesis is, the

identification and classification of the brake noises caused by faulty brakes. Various fault detection approaches are encountered in different applications of engineering. Fault diagnosis techniques can be classified as hardware redundancy and analytical redundancy (Hwang, 2011). Clonal Selection Classification (CSCA), Decision Tree Classifier (DTC), Current Ripples (CR) in electric parking brakes (EPB) are recent methods used for solution of these kind of engineering problems.

Analyzing sound signals (noise) may be an appropriate approach in detection of faulty brakes. Jegadeeshwaran and Sugumaran monitored a hydraulic brake system through vibration analysis. In this work, a Clonal Selection Classification Algorithm (CSCA) for brake fault diagnosis has been utilized (Jegadeeshwaran, 2015). Signals were acquired using a piezoelectric transducer and statistical parameters extracted from the vibration signals were evaluated. The same authors studied fault diagnosis of hydraulic brake system by means of “Machine learning approach”. They evaluated a number of statistical parameters namely standard error, kurtosis, sample variance, skewness, standard deviation, minimum, maximum, count, mean, median and range (Jegadeeshwaran, 2015).

Liu and co-workers proposed a Support Vector Machine (SVM) framework for fault detection in electro-pneumatic braking system of High Speed Trains (HSTs). The proposed framework consisting of feature and vector selection, model construction and decision boundary is validated on 15 public datasets in comparison to three of the most popular SVM models for unbalanced data (Liu, 2017).

Investigation of brake noise is also another promising way, which mostly requires time-frequency analysis together. Rhee and colleagues classified brake noise into two major categories; (a) low frequency rigid body vibration (about 100 - 1000 Hz), called brake roughness, judder, moan or groan; (b) medium and high frequency vibration (about 1000 - 18 000 Hz), called squeal or squeak. Every single brake noise has peerless characteristics and thus probably unique excitation mechanisms (Rhee, 1989). Some of the brake noises, which are both reported by the drivers and experimentally verified, could be solved by readjustments on operating conditions and optimizations on brake components such as brake pad/shoe assemblies.

A study from Delphi Chassis Systems, agrees with Rhee and his friends and they showed that this type of noise is induced by friction substance excitation at the rotor and lining interface (Dunlap, 1999).

There are six different mechanisms of squeal generation offered in the literature namely; stick-slip, negative friction – velocity slope, sprag-slip, modal coupling, splitting the doublet modes and hammering (Ghazaly, 2014).

Gajre and Talbar have analyzed vibration data acquired from a brake using quantitative features like standard deviation, mod, median, skewness and classified these features with a fuzzy logic algorithm (Gajre, 2016).

Hongquan and his co-workers have investigated brake cylinder pressure sensor fault and gas leakage fault where a cylinder and a pipe together (Zhou, 2017).

In a review article where vibration and noise signals are mostly investigated, Shannon entropy coefficients of noise data recorded from internal combustion engine have been given into artificial neural network and the success rate has been more than 95 % (Henriquez, 2014).

Lei and his friends searched vibration data acquired from shaft in time-frequency domain with adaptive neuro-fuzzy inference system (ANFIS) approach, and obtained 100 % success using 140 train and 70 test data (Lei, 2008).

Discrete Wavelet Transform (DWT) method has been used since the early 2000s, a group of researchers have used this technique in order to detect faults of ball bearing race (Prabhakar, 2002). Several approaches are offered in literature, such as usage of good heat dissipation materials or suitable friction plate in order to reduce friction rooted physical affects (Jin, 2011) but these recommendations are not very effective for all cases, since every noise signal has unique characteristics.

By Wu and Liu, DWT has been used to detect faults in an internal combustion engine and feature selection technique based on energy spectrum, in order to categorize types of faults.

By a detailed literature search, it is concluded that analyzing sound signals (noise) may be an appropriate approach for error detection.

1.4. Brake Systems

The brakes can be classified considering following parameters;

By source of power,

By method of application,

Considering method of operation,

According to braking contact and applied brake force.

According to the source of power, the brakes can be listed as mechanical, hydraulic, vacuum, magnetic, and electrical or air brakes. With respect to method of application, they are encountered as foot brakes, parking or hand brakes. They can also be listed as manual, power operated or servo. According to the braking contact they may be internal-expanding brakes or external-contracting brakes. On the basis of action the brakes are front wheel or rear wheel brakes. Finally, brakes can also be classified as single acting or double acting ones.

Most of the automobiles we see at the traffic every day, are using an antilock brake system (ABS) whereas semi-trucks and trailers use pneumatic brake systems.

In a disc brake the hydraulically linked calipers squeeze pairs of pads against a disc in order to create friction that slows down the rotation. The released energy is converted into heat that must be dispersed (Halderman 1996). In case of drum brakes, the stopping power arises from friction between the pads and a brake drum.

Hydraulic braking systems use the hydraulic pressure to force the brake shoes. They may be single circuit or dual circuit systems. It is an application of Pascal's Law.

The brake-by-wire technology controls the brakes by electrical means. This mechanism is also linked to the hydraulic pump system and when brake pedal is pushed the information from electronic wires is sent to the cars computer where the applied force is calculated.

Antilock Braking System (ABS) consists of an electrical control unit, a hydraulic actuator and an individual wheel speed sensors. These components work together to prevent brakes from locking up.

In case of air brakes hydraulic fluid is replaced by air to activate a standard disc brake. This kind of brakes are mostly used in buses and lorries.

As discussed above, braking is one of the most important tools we use every day and due to developing technology braking systems are getting smarter, safer and more complex. This complexity poses some issues as, noise and vibration defaults. From many drivers and operators, from the simplest passenger car to engineering vehicles, countless complaints due to noise and vibration have been reported not only from brakes but also from bearings, rotors and engines. These complaints led manufacturers and researches to study in the fields of fault detection using sound processing techniques. The fundamental motivation behind this thesis is to add a constructive perspective to this area for those who would like to investigate fault detection of brakes or other mechanical components in a moving vehicle.

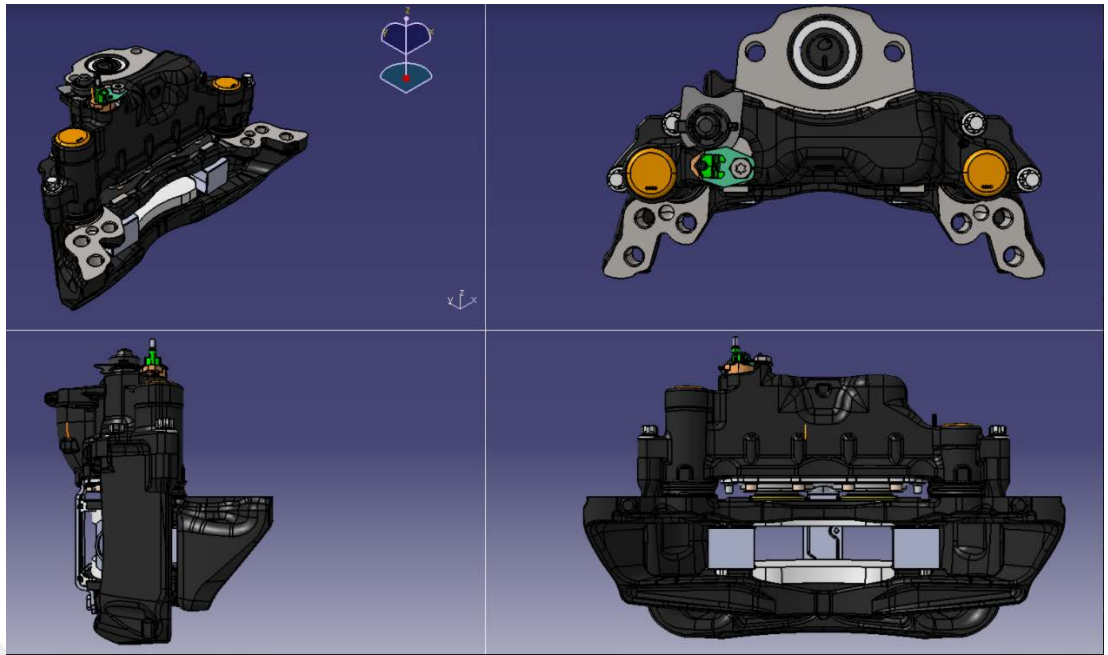


Figure 1.1. Air Disc Brake

1.5. Outline of Thesis

In Chapter 1, a literature review has been given about related works with similar techniques. Inspired by these works, outline of this thesis has been formed.

Chapter 2 includes fundamental ideas behind the Fourier Transform (FT) and theory of Wavelet Transform (WT), with the advantages and disadvantages of these signal processing methods.

In Chapter 3, time domain, frequency domain and time-frequency domain analysis of brake signals have been performed. The corresponding outputs have been given by graphics and tables.

In Chapter 4, the outputs of the complete analysis have been argued on. Future search, expectation from further investigations have been written.

CHAPTER 2

TIME, FREQUENCY AND TIME-FREQUENCY DOMAIN TECHNIQUES

In this chapter, concepts of Fourier Transform and Wavelet Transform will be given in detail.

2.1. Fourier Series and Fourier Transform

Fourier Transform (FT) is undoubtedly one of the most important mathematical developments in 20th century. In practice, periodic signals are commonly used such as square wave, triangular wave or sinusoid and so on. In order to analyze these signals in terms of frequency, Fourier Series (FS) expansion is used. This approach claims that, any periodic signal can be shown by Fourier series which includes the sum of a series of sine and/or cosine functions plus a direct current (DC) term. FS has 3 different forms; first one is sine-cosine, second one is amplitude-phase and third one is complex exponential (Tan, 2013). In this thesis, amplitude–phase form FT has been used while investigating braking intervals.

FT is a commonly used mathematical tool which enables the frequency spectral analysis for a non-periodic signal. It is defined as,

$$X(\omega) = \int_{-\infty}^{\infty} x(t)e^{-j\omega t} dt, \quad (1)$$

and the inverse Fourier Transform is given as,

$$x(t) = \frac{1}{2\pi} \int_{-\infty}^{\infty} X(\omega)e^{j\omega t} d\omega, \quad (2)$$

where $x(t)$ denotes a non-periodic signal and $X(\omega)$ represents the FT of the $x(t)$, given in equation (1) and (2). This spectrum is a complex function that can be easily written as

$$X(\omega) = |X(\omega)|\angle\phi(\omega), \quad (3)$$

where $|X(\omega)|$ is the amplitude of the continuous spectrum and $L\phi(\omega)$ represents the related phase.

Discrete Fourier Transform (DFT) basically transforms any time domain signal to the frequency domain by summing at instants separated by sample times, calculated by;

$$X(k) = \sum_{n=0}^{N-1} x(n)e^{-j2\pi n/N} = \sum_{n=0}^{N-1} x(n)W_N^{kn}, \quad (4)$$

for $k=0, 1, \dots, N-1$,

Where $x(n)$ is the time domain signal, namely sequence and $X(k)$ refers to the DFT coefficients. n Represents the sample number of the sequence whereas k denotes the frequency index.

Where W_N is given as a form of Euler's identity,

$$W_N = e^{-j2\pi/N} = \cos\left(\frac{2\pi}{N}\right) - j \sin\left(\frac{2\pi}{N}\right), \quad (5)$$

A computationally efficient implementation is of DFT is called as Fast Fourier Transform (FFT) and it is widely used for obtaining frequency spectrum of the digital signals.

$$X[k] = \sum_{n=0}^{N/2-1} x_{even}[n]W_{N/2}^{kn} + W_N^k \sum_{n=0}^{N/2-1} x_{odd}[n]W_{N/2}^{kn}, \quad (6)$$

$$X_{even}[k] + W_N^k X_{odd}[k], \quad (7)$$

Where $X_{even}[k]$, $X_{odd}[k]$ are the $\frac{N}{2}$ point DFT transforms of the even and odd components of $x(n)$ respectively. In the equation above, N point DFT has been divided into $\frac{N}{2}$ point DFTs. The divide and obtain procedure provides a fast and sufficient analysis.

2.1.1. Disadvantages of Fourier Transform

FT shows, what frequency components are present in the signal, which means that the time information is lost. It is suitable for stationary signals like, white Gaussian Noise. However, sometimes it is required to know, where in time did this frequency component occur?

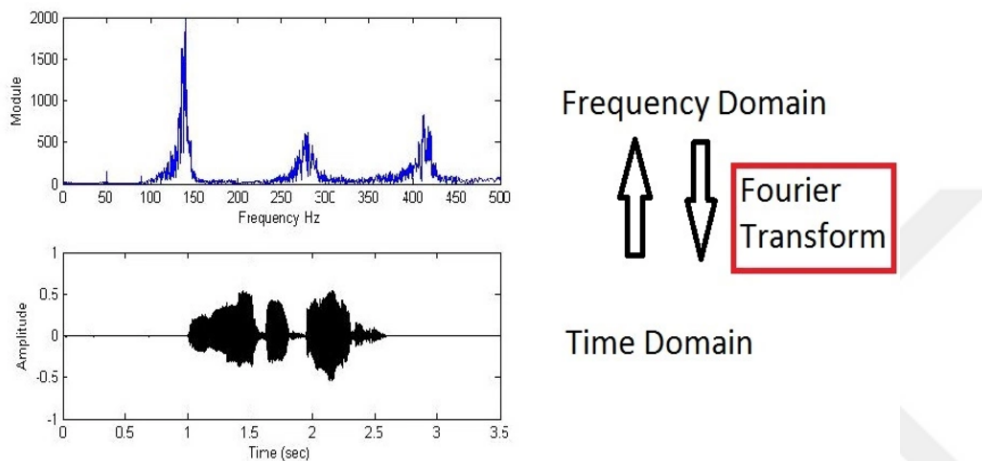


Figure 2.1. From time domain to frequency domain (Dallas, 2014)

In Figure 2.1, the representation does not bring out how the frequency contents of the signal change within time; or it does not give information if the two main frequencies are continuously existing or only at particular intervals. Since the temporal structure of the signal cannot be observed, the advantages of the Fourier transform is somehow bounded.

In figure 2.2, a non-stationary signal has been shown both in time and frequency domain separately. It is clear that, by applying FT, a lot of information about the signal is lost. FT is not suitable enough to analyze nonstationary signals. A different signal processing approach which is able to handle nonstationary signals, is needed.

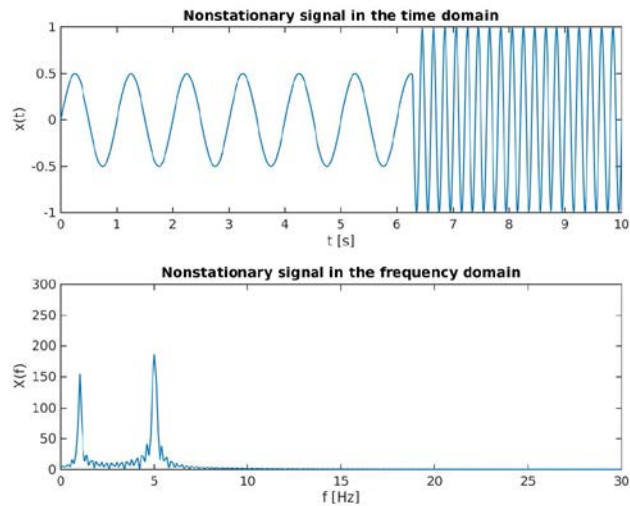


Figure 2.2. Representation of a nonstationary signal, both in time and frequency domains (Heuser, 2014)

2.1.2. Short Time Fourier Transform

In order to deal with the limitations of the Fourier transform, a Fourier-like technique is used by Dennis Gabor in 1946. An investigation window of particular length, which glides throughout the signal, along the time axis, works as a “time localized” FT. This approach introduced by Dennis Gabor, led to the concept of short-time Fourier Transform (STFT).

In Figure 2.3 and 2.4, there is a sliding window function $g(t)$ centered at time t . For every single t , a time localized FT is done on $x(t)$ within the window. The analysis window displaces along the time axis, repeating another FT. Following sequential operations, it is possible to obtain the FT of the entire signal. In figure 2.4. the signal range under the window is assumed to be almost stationary. Using STFT, a time domain signal can be easily decomposed into a 2D time-frequency representation.

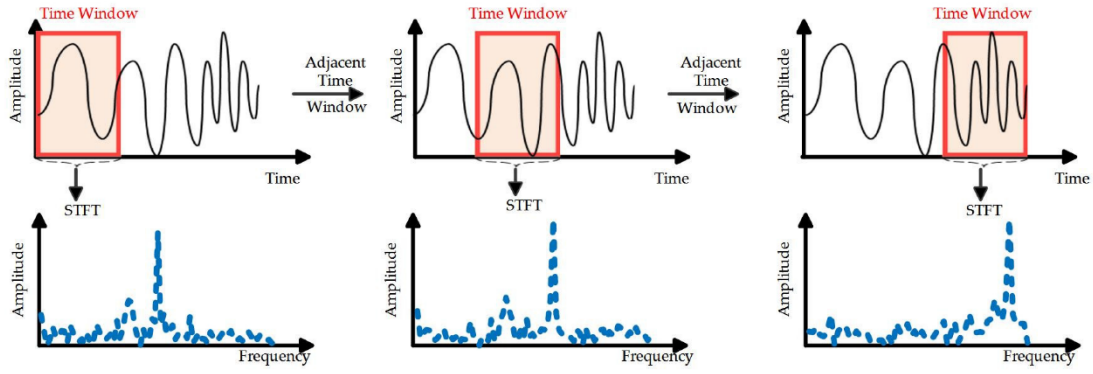


Figure 2.3. Sliding window function in frequency domain, (Kumar, 2017)

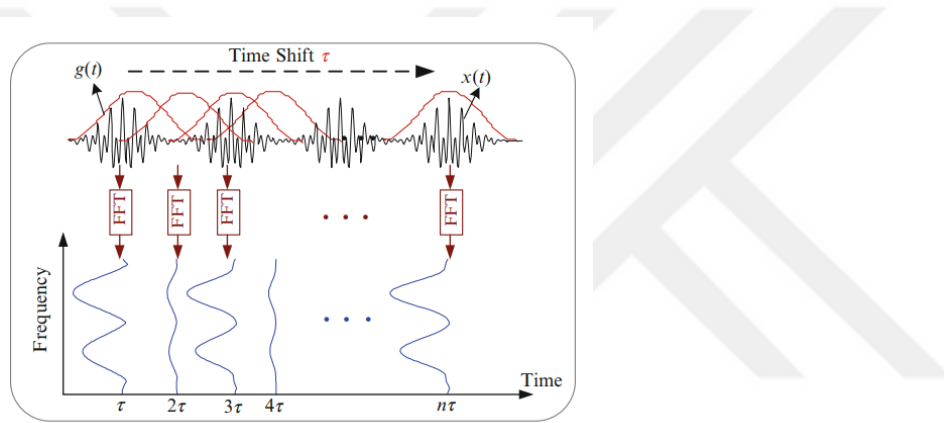


Figure 2.4. STFT application, (Gao, 2011)

Mostly, higher resolution provides greater separation of the constituent components of signal, the time and frequency resolutions of the STFT technique must not be chosen arbitrarily at once according to the uncertainty principle of Cohen.

Particularly, the multiplication of the time and frequency resolutions is lower bounded by

$$\tau \cdot \Delta f \geq \frac{1}{4\pi}, \quad (8)$$

where $\Delta\tau$ and Δf denotes time and frequency resolutions, respectively.

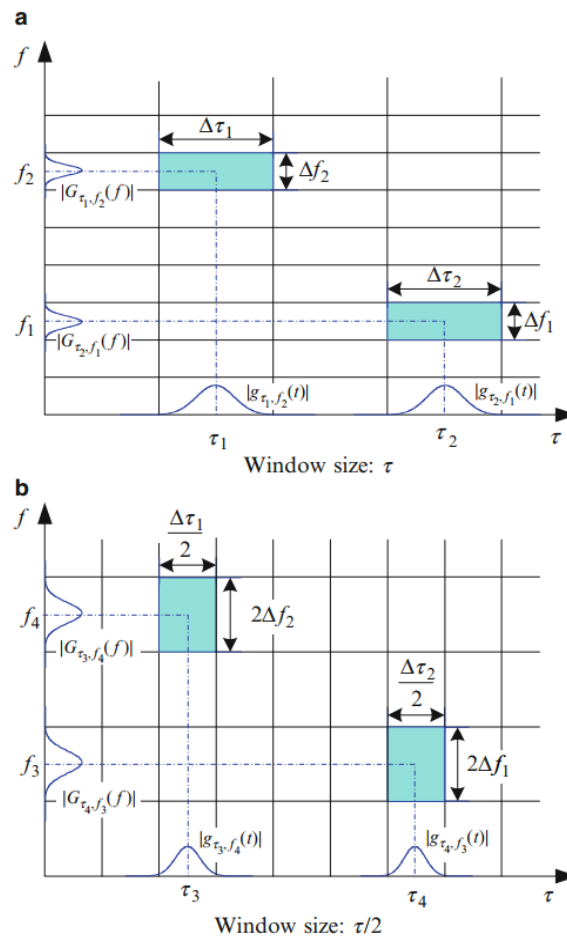


Figure 2.5. STFT window sizes representation, (Gao, 2011)

In figure 2.5, it is shown that regardless of the window sizes, the product of $\Delta\tau$ and Δf are always equal because of Uncertainty Principle. Although inspecting both the time and frequency information at the same time was a great development, fixed window size had continued to be challenge.

When the demands of the customers and the developments in technology almost met during 1900s' and early 2000s', terms of the day entailed engineers to design more advanced electromechanical systems hence the fault diagnosis got harder and as a consequence signal processing techniques developed eventually. Conclusions of researches showed that observing time and frequency information at the same time, with a higher resolution could be a pioneering approach in order to discriminate obscure faults clearly. In the early 1980's, a French geophysicist called Jean Morlet,

claimed a new concept, wavelets of constant shape. Contrary to the STFT approach, where the window size is fixed, the wavelet technique allows flexible window sizes while investigating different frequency components within a signal (Mallat, 1998).

Wavelet transform is an alternative technique to the STFT in order to solve resolution problem. It is pretty similar to STFT, only multiplied with a function of wavelet. Multiresolution analysis has the following advantages,

1. The signal can be analyzed with different resolutions at different frequencies.
2. At high frequencies, it gives poor frequency resolution and good time resolution.
3. At low frequencies, it gives poor time resolution and good frequency resolution.
4. More appropriate for higher frequency components of short duration and for lower frequency components for longer duration.

In figure 2.6, a simple wavelet application representation is given. While applying wavelet transform, you simply cut the signal up into smaller signals, showing the same signal only corresponding to varying frequency bands. Solely, keeping the frequency at the exact time interval.

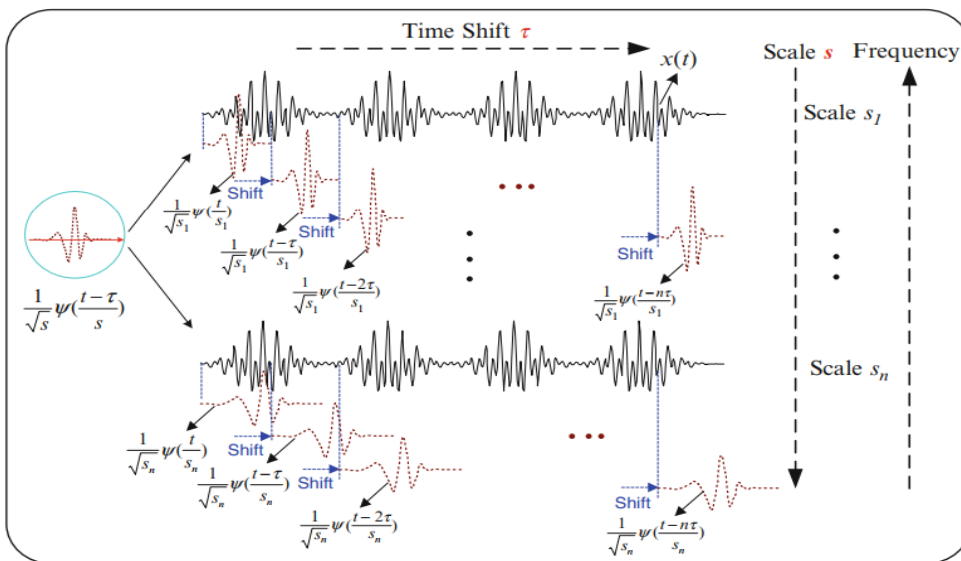


Figure 2.6. Wavelet application, (Gao, 2011)

2.2. Wavelet Analysis

Wavelet refers to a small wave which has to decay within a short time interval and in a very small area. The concept of Wavelet expands to early 1800s, the discovery of superposing sines and cosines by Joseph Fourier. Wavelet is an efficient and multipurpose tool which is widely used for signal processing. It is appropriate for the analysis of non-stationary or transient data.

Wavelets can be used to extract information from a large variety of data, extending from financial data to audio or images processing.

In order to perform a wavelet transform, a wavelet function $\psi(t)$ is needed which is a specifically localized and satisfies certain mathematical criteria.

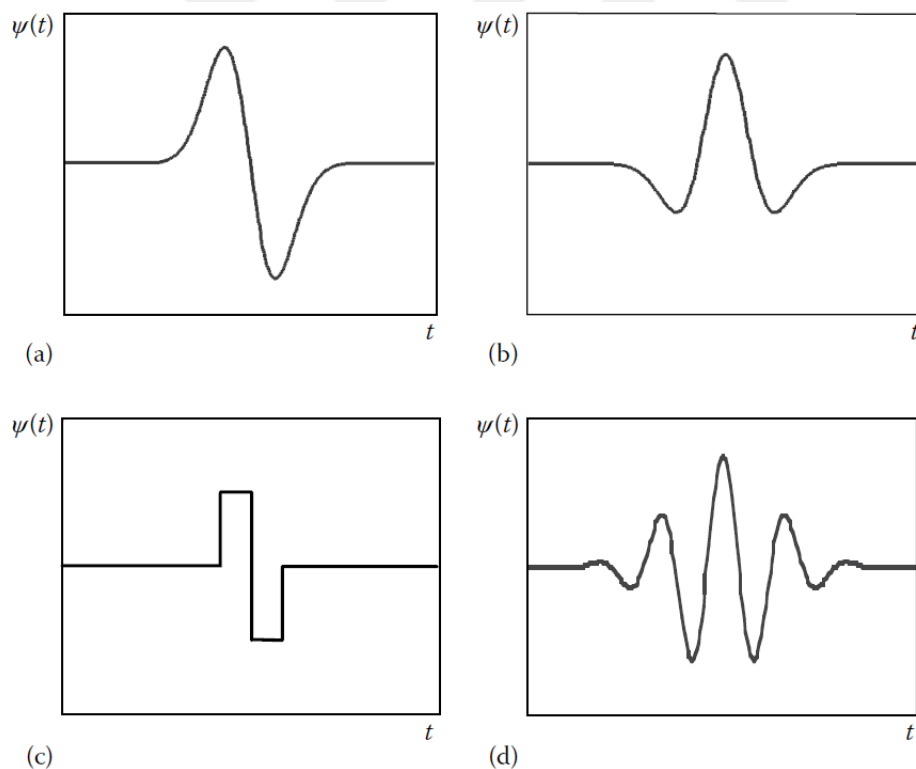


Figure 2.7. Four common wavelets: (a) Gaussian wave (first derivative of a Gaussian). (b) Mexican hat (second derivative of a Gaussian). (c) Haar. (d) Morlet (real part).

Although, there are many types of wavelets, the tricky part is to choose the right one for you. What you expect in the analysis and the behavior of the signal are two main topics that you consider while choosing your wavelet.

2.2.1. Requirements for the Wavelet

A wavelet function has to satisfy certain mathematical criteria,

1. A wavelet must have finite energy.

$$E = \int_{-\infty}^{\infty} |\psi(t)|^2 dt < \infty, \quad (9)$$

2. If $\hat{\psi}(\omega)$ is the Fourier transform of $\psi(t)$

$$C_\varphi = \int_0^{\infty} \frac{|\hat{\psi}(\omega)|^2}{|\omega|} d\omega < \infty, \quad (10)$$

must be satisfied. It means $\hat{\psi}(0) = 0$, namely $\psi(t)$ must have a zero mean. C_φ refers to the admissibility constant.

3. For complex wavelets, the Fourier Transform (FT) must be real and the negative frequencies must disappear (Addison, 2017).

2.2.2. The Energy Spectrum of the Wavelet,

If a wavelet satisfies admissibility condition (equation (10)), it is called band-pass filter. The frequency of the wavelet versus squared magnitude of the FT gives the energy spectrum is given by

$$E_F(\omega) = |\hat{\psi}(\omega)|^2, \quad (11)$$

Denoted by f_c , the standard deviation of the energy spectrum is as follows,

$$f_c = \sqrt{\frac{\int_0^{\infty} f^2 |\hat{\psi}(\omega)|^2 df}{\int_0^{\infty} |\hat{\psi}(\omega)|^2 df}}, \quad (12)$$

The total energy of a wavelet is finite, as a result of Parseval's Theorem.

$$E = \int_{-\infty}^{\infty} |\psi(t)|^2 dt, \quad (13)$$

In another way, the area under the energy spectrum also gives the total energy.

$$E = \int_{-\infty}^{\infty} |\hat{\psi}(\omega)|^2 d\omega, \quad (14)$$

Hence, applying Parseval's theorem, we expect this for any function.

$$\int_{-\infty}^{\infty} |\psi(t)|^2 dt = \int_{-\infty}^{\infty} |\hat{\psi}(\omega)|^2 d\omega, \quad (15)$$

Practically, the wavelet function has unit energy since it is normalized.

2.2.3. Wavelet Transform

Right after choosing an appropriate mother wavelet, to make it more flexible and amenable, there are two basic manipulation options, "dilation" and "translation". While the dilation refers to squeezing and stretching, the translation is the displacement (movement) along the time axis.

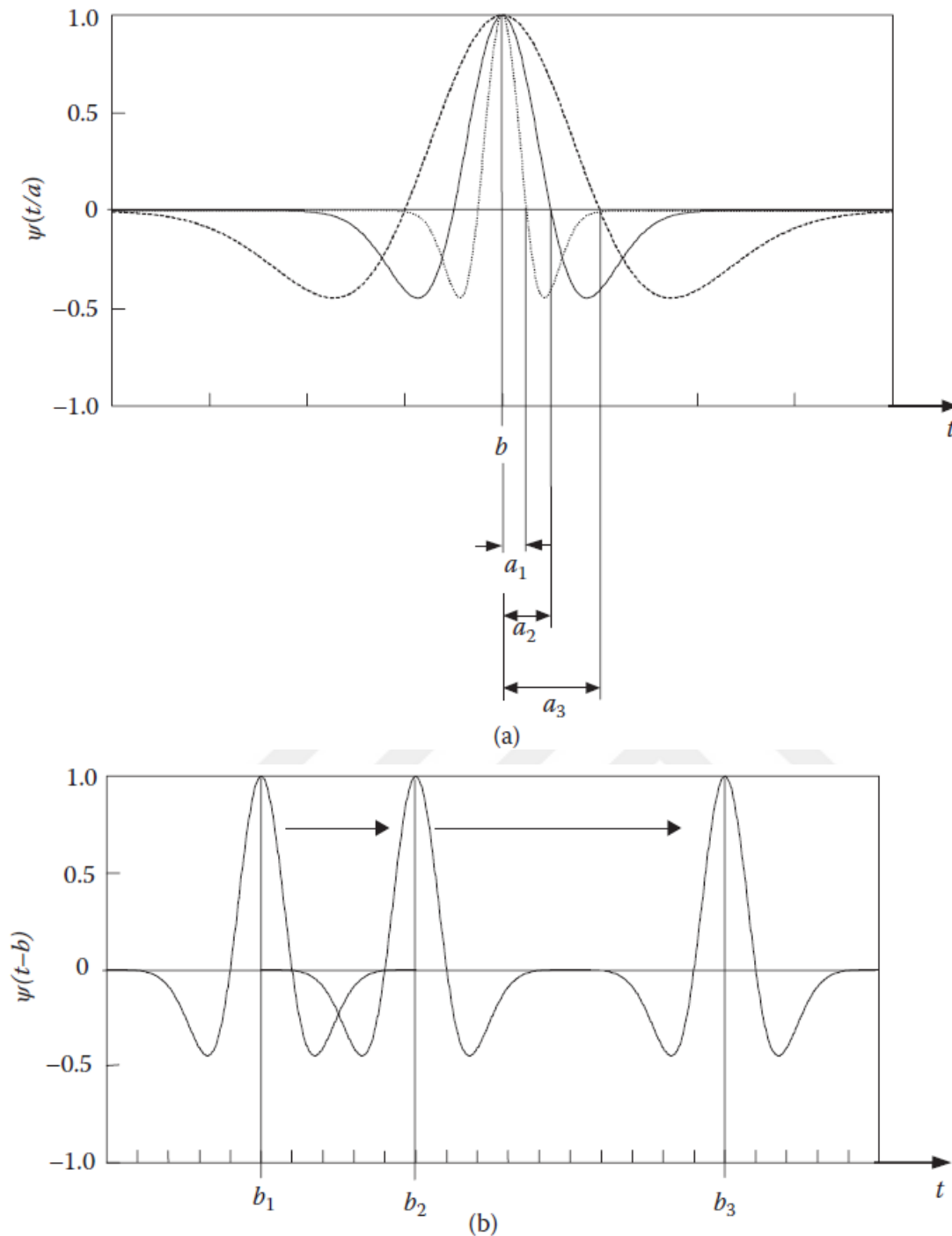


Figure 2.8. Dilation and translation of a wavelet: **(a)** Stretching and squeezing a wavelet: Dilation ($a_1 = a_2/2$; $a_3 = a_4 \times 2$). **(b)** Moving a wavelet: Translation.

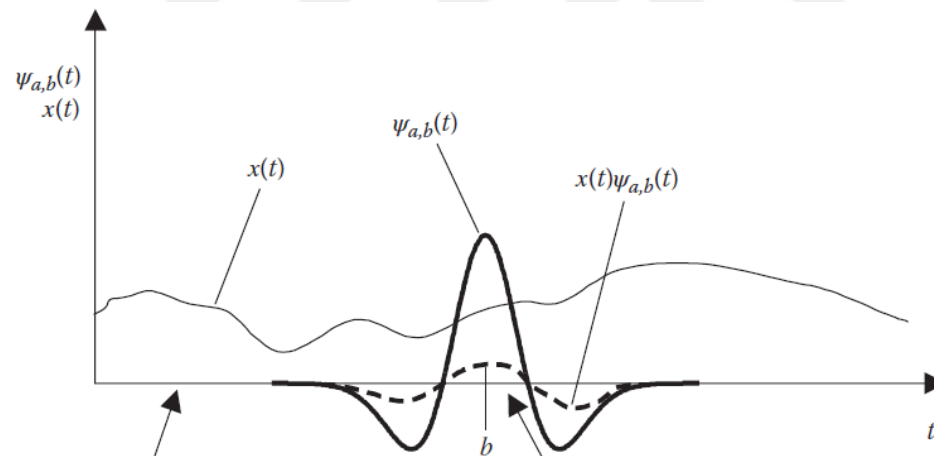
In figure 2.8a, the wavelet is squeezed and stretched respectively, half and double its original width on the time axis. The dilation variable is denoted by “a”. The translation from b_1 via b_2 and b_3 , shift along the time axis is denoted by “b” in general (Addison, 2017).

$$T(a, b) = \frac{1}{\sqrt{a}} \int_{-\infty}^{\infty} x(t) \psi^* \left(\frac{t-b}{a} \right) dt, \quad (16)$$

The $x(t)$ function in equation (16) could be a financial index, a heart beat, an audio signal or even a seismic signal. In this equation, the product of the signal (audio and vibration in this work) and the mother wavelet are integrated, during the signal range. Mathematically, the convolution operation has been performed. The normalized wavelet is simply given by,

$$\psi_{a,b}(t) = \frac{1}{\sqrt{a}} \psi \left(\frac{t-b}{a} \right), \quad (17)$$

Fourier transform values of complex wavelets, (in other words analytic wavelets) are zero for negative frequencies due to the 3rd requirement of the wavelet. Implementing this information, by choosing complex wavelets, the phase and amplitude components of a signal can be easily separated.



(a)

Near zero values of the wavelet here lead to near zero contributions to the transform in regions far from b

Features in the signal are highlighted by the wavelet in the vicinity of b

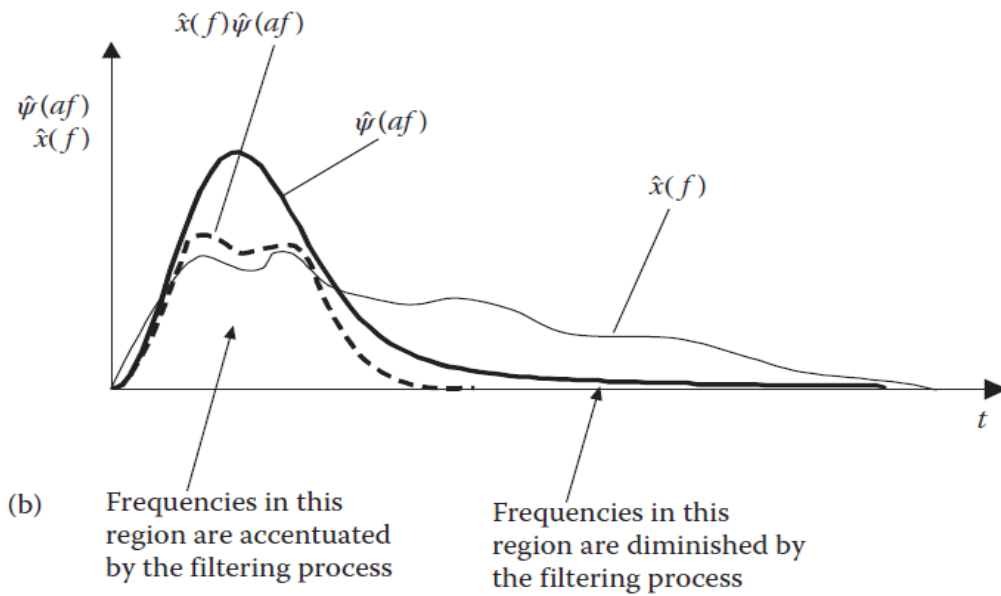


Figure 2.9. Schematic representation of the wavelet transform in its time and frequency representations: (a) The convolution operation of the wavelet function with the signal. (b) The obtained convolution in (a) is shown in the frequency domain contains a product of the signal Fourier transform and the wavelet Fourier transform (Addison, 2017).

2.2.4. Inverse Wavelet Transform

The inverse wavelet transform is defined as,

$$x(t) = \frac{1}{c_\varphi} \int_{-\infty}^{\infty} \int_0^{\infty} T(a, b) \frac{\psi_{a,b}}{a^2} da db, \quad (18)$$

By integrating over dilation and translation parameters a and b , the wavelet transformed version turns in to original signal. Instead of using all dilation parameters (a scales), integration over a limited range of dilation parameters conclude as basic filtering. In fig. 2.10a.b.c, three components of a signal are given, in fig 2.10d the addition of these components shows the original composite signal.

The plot of transformed signal is given in fig 2.10e. The abrupt burst of high frequency noise is also clearly obtained in the transformed signal.

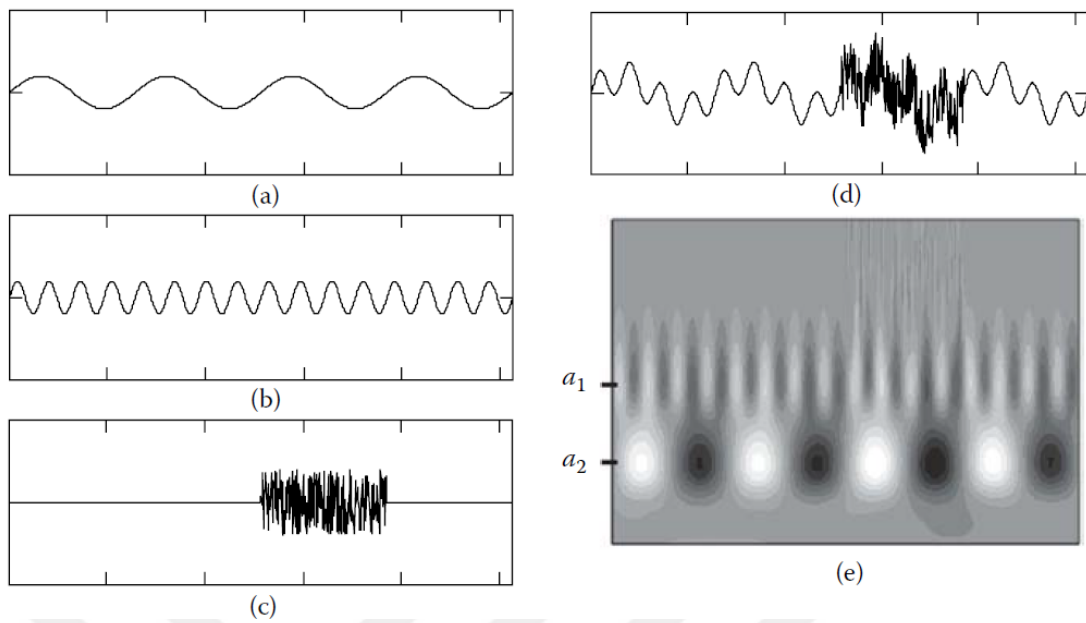


Figure 2.10. The signal and the plot of its transformation. (a) Sinusoidal waveform. (b) Sinusoidal waveform. (c) Abrupt high frequency noise. (d) Addition of (a), (b) and (c). (e) The transformation plot of the embodied signal (Addison, 2017).

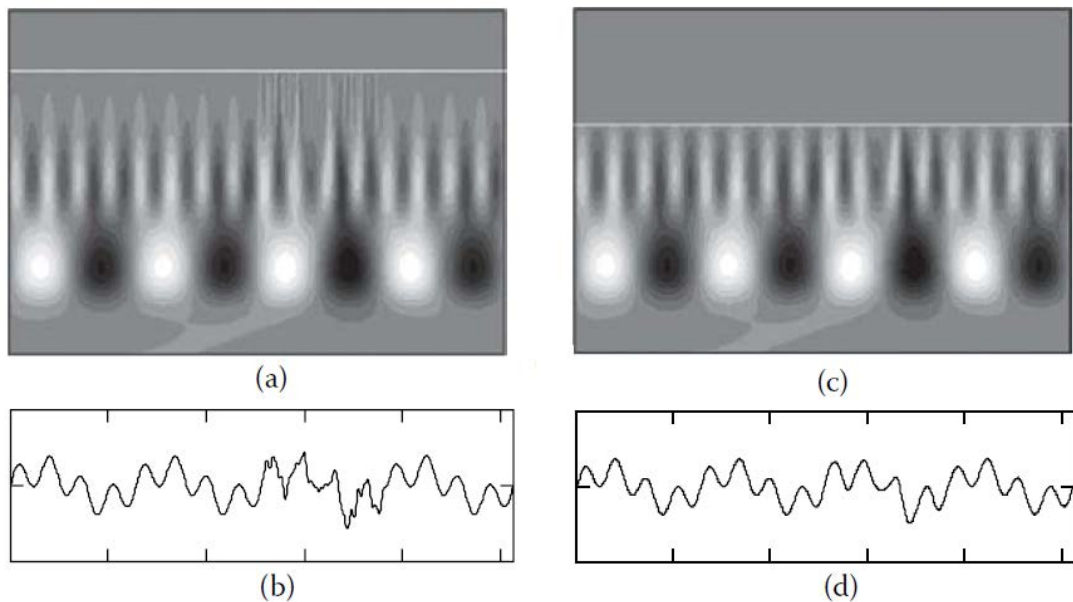


Figure 2.11. Filtering of the embodied signal by wavelet. (a) High frequency components above the line are eliminated in 2.10e. (b) Rebuild signal using the plot in

(a). (c) Relatively small scale components are removed in fig 2.10e. (d) Rebuild signal using the plot in (c). Rebuilding the signal, over a range of dilation parameters (a), $a^* < a < \infty$. The White lines in the figures, represents the cut off scale. As the scale (dilation parameter, cut off) increases, the reduction of high frequency noises are more apparent (Addison, 2017).

2.2.5. Power Spectra and Wavelet Based Energy

The total energy contained in a signal is defined as,

$$E = \int_{-\infty}^{\infty} |x(t)|^2 dt = \|x(t)\|^2, \quad (19)$$

Known that, only finite energy is useful, by using dilation and translation parameters, 2-D wavelet energy density function can be written as,

$$P_s(a, b) = |T(a, b)|^2, \quad (20)$$

$P_s(a, b)$ plot is called scalogram.

2.2.6. Scalogram

Scalogram which represents the local time-frequency intensity can be written as,

$$P_s(a, b; \psi) \triangleq |W_s(a, b; \psi)|^2, \quad (21)$$

By using wavelet coefficients. Scalogram shows, how energy of the signal is distributed over time-frequency plane.

2.2.7. Complex Morlet Wavelet

Morlet Wavelet

A Complex Morlet wavelet is the product of the sine wave with a Gaussian function. Based on this, a Complex Morlet is the multiplication of a complex sine wave with a Gaussian function. The FT of complex or analytic wavelets are zero for (-) frequencies. Using this kind of complex wavelets, it is possible to separate the phase and the amplitude components for a signal. Theoretically, if we take the FT of the Mexican Hat Wavelet (MHW), then fix the negative components in the frequency domain to 0, finally applying an IFT, we obtain a complex MHW.

The Morlet Wavelet is commonly used and defined as,

$$\psi(t) = \pi^{-1/4} \left(e^{i2\pi f_0 t} - e^{-\frac{(2\pi f_0)^2}{2}} \right) e^{-\frac{t^2}{2}}, \quad (22)$$

where the central frequency is denoted by f_0 . The second term in the brackets neutralizes the contribution which comes from non-zero mean of the complex sinus function of the first term. Thus named as correction term which is practically, negligible for $f_0 > 0$ and can be ignored. A simpler form of complex Morlet is written as,

$$\psi(t) = \frac{1}{\pi^{1/4}} e^{i2\pi f_0 t} e^{-\frac{t^2}{2}}, \quad (23)$$

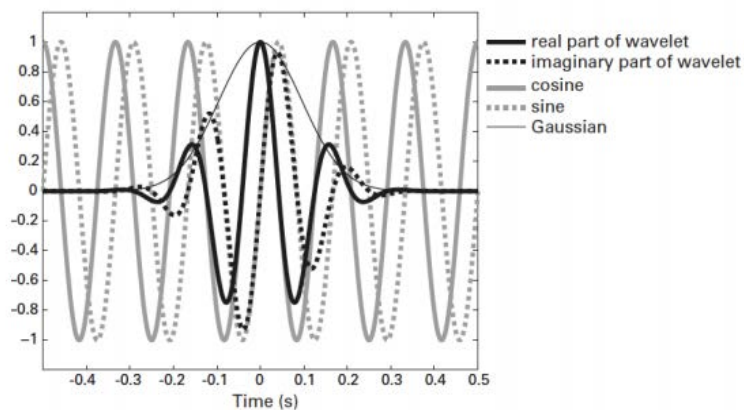


Figure 2.12. Morlet Wavelet, (Addison, 2017)

Given in figure 2.13, morlet wavelet, actually, is a complex sine wave under a Gaussian envelope. The complex sinusoidal waveform comes from equation (24) whereas the term $e^{-t^2/2}$ bounds the waveform and has unit standard deviation. The $\pi^{1/4}$ is the normalization term which guarantees that wavelet has unit energy. The FT of the Morlet Wavelet is given as,

$$\hat{\psi}(f) = \pi^{1/4} \sqrt{2} e^{-\frac{1}{2}(2\pi f - 2\pi f_0)^2}, \quad (24)$$

The energy spectrum of the Morlet is written as,

$$|\hat{\psi}(f)|^2 = 2\pi^{1/2} e^{-(2\pi f - 2\pi f_0)^2}, \quad (25)$$

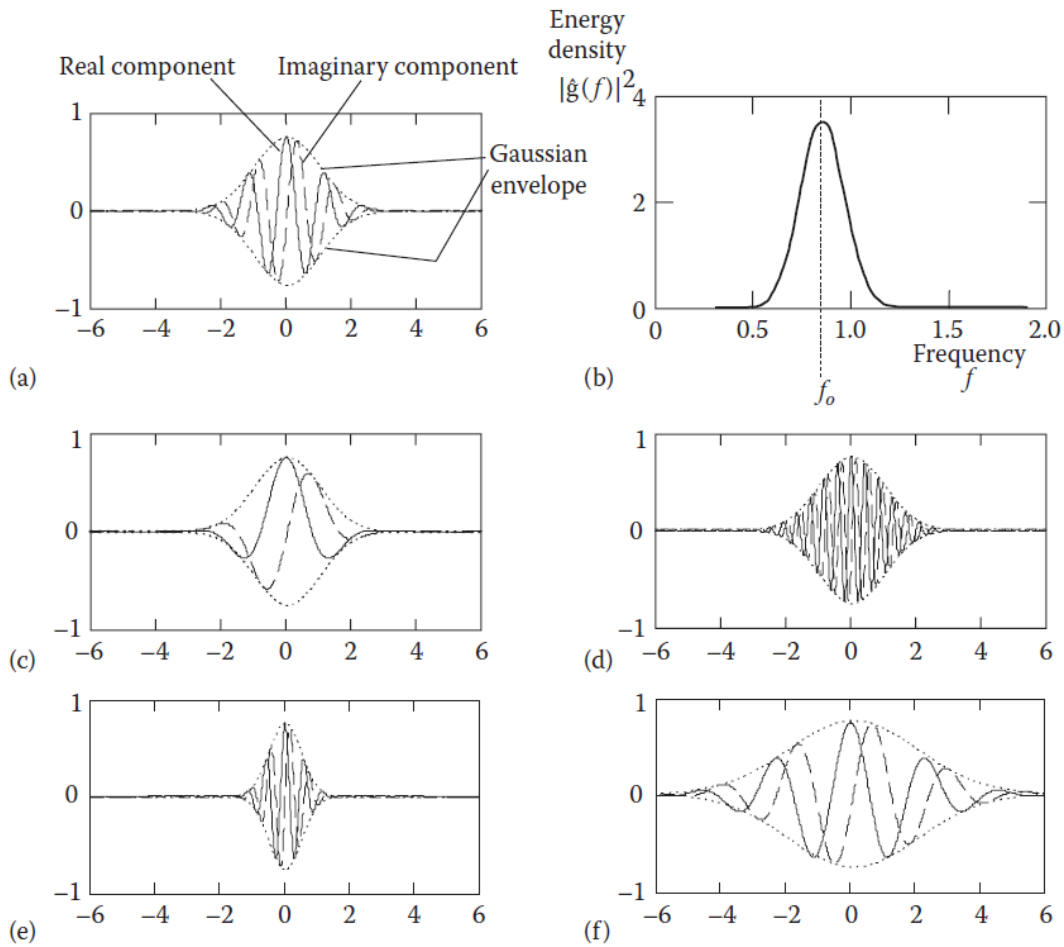


Figure 2.13. (a) the morlet wavelet, (b) the energy spectrum of the Morlet is given.

In figure 2.13 c 2.13 d 2.13 e 2.13 f, various plots are given for different center frequencies and scales, (Addison, 2017).

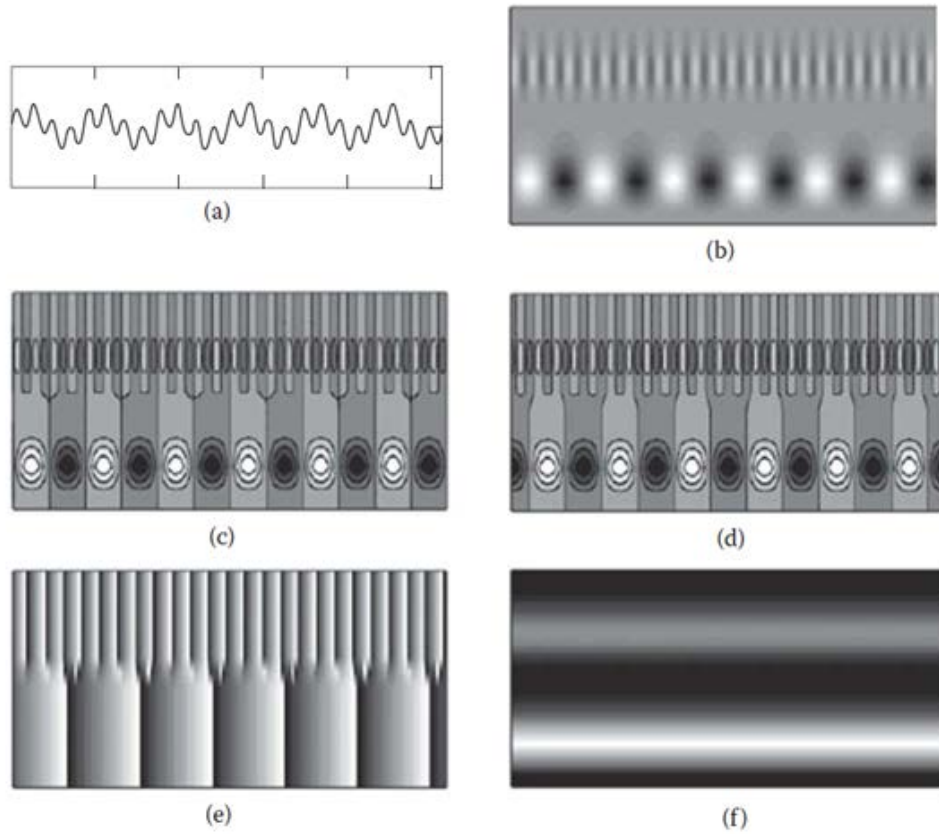


Figure 2.14. Morlet wavelet analysis of a two-component sinusoidal waveform.

In the figure above, an analysis of a two component sinusoidal waveform, using Morlet Wavelet (Addison, 2017), with a center frequency of $f_0=0.849$ is given. The real part of the wavelet transform $Re\{T(a,b)\}$ the signal is given in 2.14b whereas the contoured and shaded version of the real part of the wavelet transform is given in 2.14c. Duly, two wavelet components are obvious as small waves, at the different scales, in fig 2.14b. The phase of the wavelet transform is given in 2.14e and the modulus is shown in 2.14f.

2.2.8. Morlet Wavelet Decomposition of a Signal

The Morlet Wavelet decomposition of a signal, which has an abrupt change in periodicity, is investigated in figure 2.15. The change in periodicity is evident on all analyses. Extracting and separating the signal into its constituent components is the goal of decomposition.

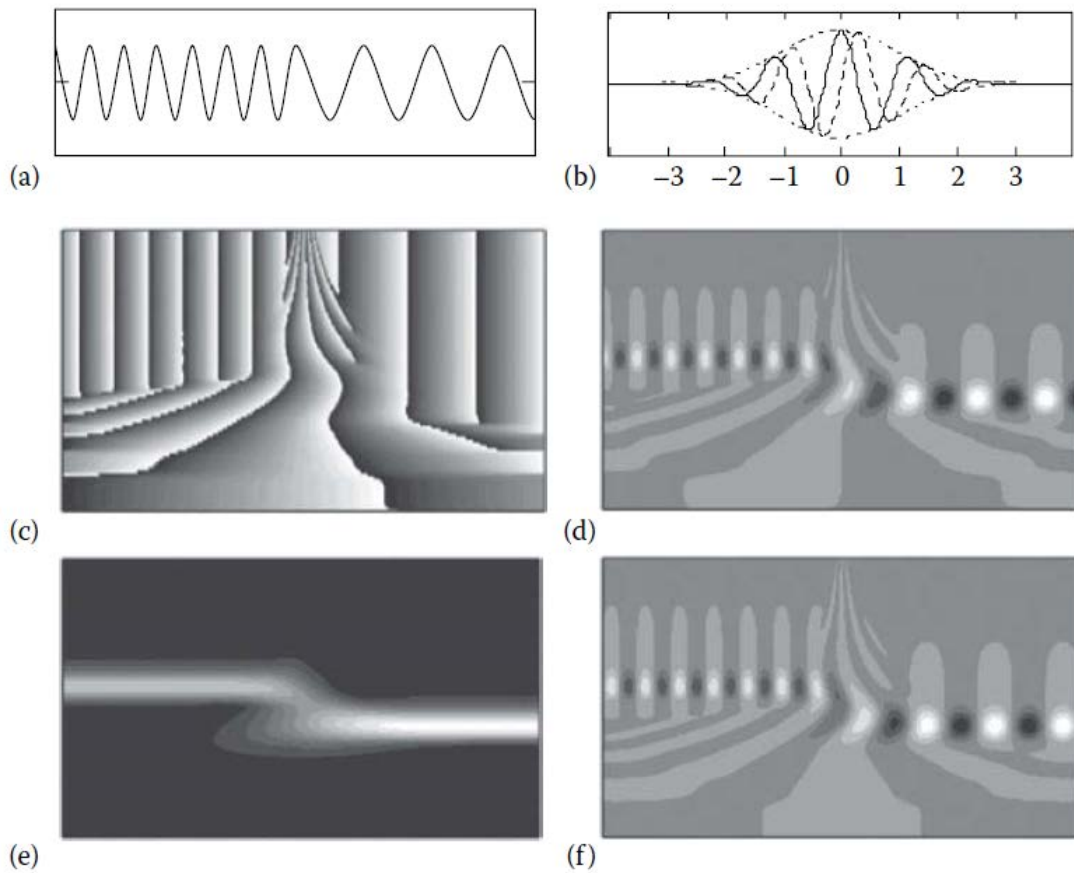


Figure 2.15. (a) Original Signal (b) Morlet Wavelet Transformation (c) Phase (d) Real part (e) modulus (f) Imaginary part of the Wavelet transform.

2.3. Discrete Wavelet Transform

It is possible to rebuild the original signal by means of infinite summations of discrete wavelet coefficients. This approach allows faster wavelet transformation for the quick calculation of the Discrete Wavelet Transform (DWT) and its inverse. Reconstruction of the original signal by CWT method is also possible but not as preferable as DWT because it brings out a challenge since the CWT includes too much redundant information; the reconstructed signal is an approximate representation (Addison, 2017). Forward and backward transforms of DWT are computationally efficient, meanwhile capturing all the signal's discriminative features.

The fundamental DWT is computed by following the steps below,

1. A signal is fed into a low-pass filter and a high-pass filter, namely by *father wavelet and mother wavelet*.
2. The outputs of the filters are downsampled by 2:1 ratio, which ensures that the remaining coefficients have the same dimension of the input signal. Power-of-two logarithmic selection is defined as the 'dyadic grid'.
3. First two steps are repeated until the desired component of the signal is obtained.

$$\varphi_{m,n}(t) = \frac{1}{\sqrt{a_0^m}} \varphi\left(\frac{t - nb_0 a_0^m}{a_0^m}\right), \quad (26)$$

Where the integer m denotes the wavelet dilation whereas the n refers to the wavelet translation. Explained briefly in step 2 above, a useful selection for discrete wavelet parameters a_0 and b_0 are 2 and 1, respectively in order to provide a rapid and efficient computation.

$$\varphi_{m,n}(t) = 2^{-\frac{m}{2}} \varphi(2^{-m}t - n), \quad (27)$$

Discrete dyadic grid wavelets are mostly preferred to be satisfy the feature of orthonormality. These wavelets are orthogonal in themselves and they are normalized to have unit energy given in equation below,

$$\int_{-\infty}^{\infty} \varphi_{m,n}(t) \varphi_{\acute{m},\acute{n}}(t) dt = \begin{cases} 1, & \text{if } m = \acute{m} \text{ and } n = \acute{n} \\ 0, & \text{otherwise} \end{cases}, \quad (28)$$

The major reason behind this is, the data kept in a wavelet coefficient $T_{m,n}$ is not repeated anywhere hence the perfect reconstruction of the original signal without redundancy is possible. This feature is satisfied by virtue of orthonormality where the product of each wavelet with all others equals to zero, in the same dyadic grid system since they are all perpendicular to each other.

Orthonormal wavelets have frame bounds $A = B = 1$ where the related wavelet family is said to be orthonormal basis. (A basis consists of a set of vectors in a space, where the vectors are linearly independent and they can be represented as linear combination of this set, mathematically. In other words, these vectors span the space they are in. In terms of signal processing, orthonormal wavelets namely, linearly independent vectors which can perfectly define the signal (Addison, 2017).

A signal $x(t)$ can be written as a combined series expansion with the help of approximation coefficients and the wavelet (detail) coefficients together,

$$x(t) = \sum_{-\infty}^{\infty} S_{m_0,n} \phi_{m_0,n}(t) + \sum_{m=-\infty}^{m_0} \sum_{n=-\infty}^{n_0} T_{m,n} \varphi_{m,n}(t), \quad (29)$$

In this work, wavelets of Daubechies; Db3 Db6 Db9 Db10 Db12 Db15 and Db18 are used from the wavelet family, given below,

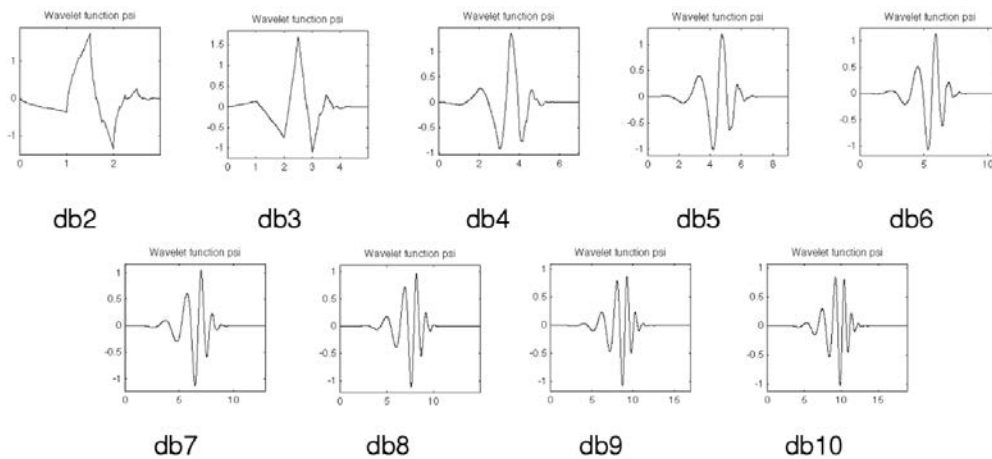


Figure 2.16. Daubechies wavelets

DWT is also known as Fast Wavelet Transformation (FWT), where coefficients of coefficients are calculated.

$$S_{m+1,n} = \frac{1}{\sqrt{2}} \sum_k c_k S_{m,2n+k} = \frac{1}{\sqrt{2}} \sum_k c_{k-2n} S_{m,k} , \quad (30)$$

$$T_{m+1} = \frac{1}{\sqrt{2}} \sum_k b_k S_{m,2n+k} = \frac{1}{\sqrt{2}} \sum_k b_{k-2n} S_{m,k} , \quad (31)$$

In equation 30 and 31, if the approximation coefficients $S_{m0,n}$ is known at a pre-defined scale, for all scales bigger than $m0$, it is possible to obtain approximation and detail wavelet coefficients, also known as multiresolution decomposition approach. In the first half of WT is applied so that wavelet coefficients are computed. Shown in figure 2.17, iterating equations 30 and 31 performs, respectively, a high-pass and low-pass filtering of the original signal, where $(1/\sqrt{2})c_k$ and $(1/\sqrt{2})b_k$ denote the filters. The low-pass filter allows only low frequency components to pass thus, smoothed signal is obtained whereas the high-pass filter permits high frequencies to pass, so that signal details are evaluated. The second half of WT consists of reconstruction algorithm (Addison, 2017).

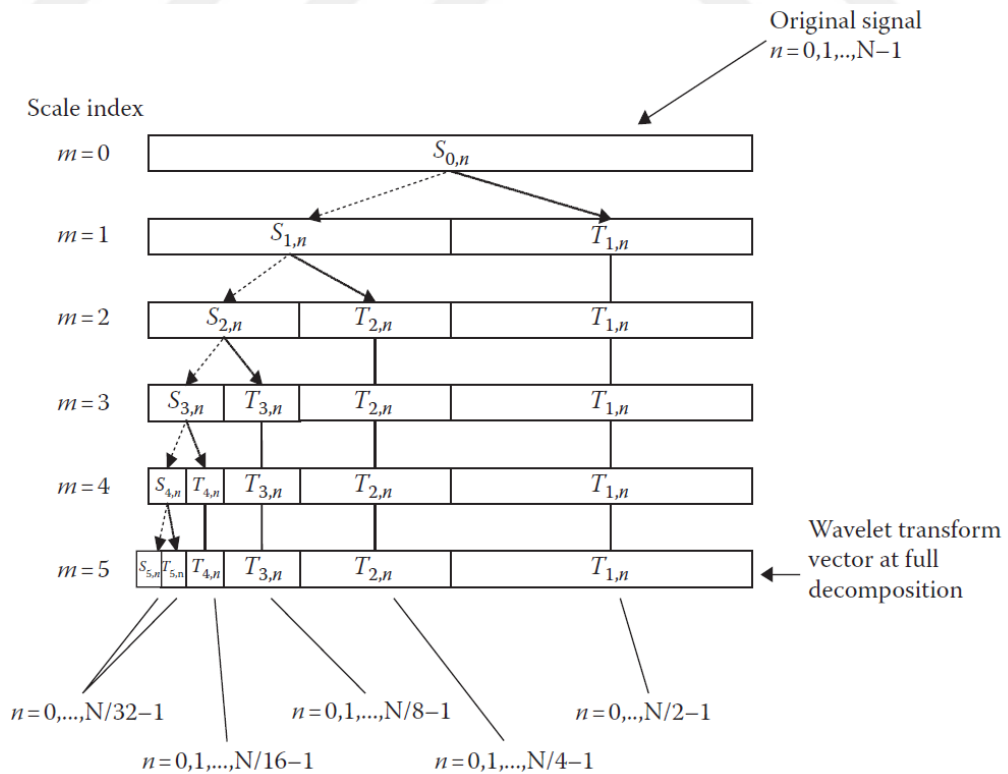


Figure 2.17. Filtering of the signal

In the figure above, the original signal is filtered by sliding the low-pass filter throughout the signal one step at a time in order to obtain the approximation coefficient $S_{1,n}$. The detail coefficients are computed the same way but only using a high-pass wavelet filter coefficients. Representation of the dissolution and insertion of the approximation and detail coefficients for every iteration within the WT vector for any input signal vector is shown above.

The wavelet transform vector after the full decomposition has the form $\mathbf{W}^{(M)} = (\mathbf{S}_M, \mathbf{T}_M, \mathbf{T}_{M-1}, \dots, \mathbf{T}_m \dots \mathbf{T}_2, \mathbf{T}_1)$ where \mathbf{T}_m denotes the sub-set including the coefficients $T_{m,n}$ at scale index m , n varies between 0 to $2M-m-1$.

DWT operation for noisy and less noisy brakes have been performed in MATLAB and related outputs are given in next chapter of the thesis.

2.4. Wavelet Ridges

Wavelet ridges indicate the points where energy rises up in scalogram matrix and converge on the instantaneous frequency of the signal within a certain resolution. In order to obtain Wavelet Ridges several methods can be found in a literature review (Özkurt, 2015). In this thesis Singular Value Decomposition (SVD) method has been applied to noise data acquired from brakes, to detect wavelet ridges.

Scalogram Matrix is defined as

$$P=[p_{mn}]_{M \times N}, \quad (32)$$

$$p_{mn} \triangleq |c_{mn}|^2 \quad (33)$$

and given below, complex Morlet Wavelet has been chosen as the mother wavelet.

$$\varphi(t) = \frac{1}{2\pi} \cdot e^{j\omega_0 t} e^{-t^2/2}, \quad (34)$$

ω represents the center frequency of the wavelet. Since it provides observation of magnitude and phase separately, it is immensely useful.

SVD based ridge detection algorithm is used in this study. The scalogram matrix $P \in \mathbb{R}^{M \times N}$ can be decomposed into singular values as

$$P = U \Sigma V^T, \quad (35)$$

Here, singular value matrix is given as $\Sigma \in \mathbb{R}^{M \times N}$ whereas orthogonal matrices are defined as $U \in \mathbb{R}^{M \times M}$ and $V \in \mathbb{R}^{N \times N}$. Since singular values ordered in descending order, when energy of the noise is assumed to be less than the energy of the signal, the matrix can be investigated in two parts.

$$\Sigma = \begin{bmatrix} \Sigma_s & 0 \\ 0 & \Sigma_n \end{bmatrix}, \quad (36)$$

$$U = [U_s \quad U_n], \quad (37)$$

$$V = [V_s \quad V_n], \quad (38)$$

$U_s \in \mathbb{R}^{M \times S}$, $\Sigma_s \in \mathbb{R}^{S \times S}$ ve $V_s \in \mathbb{R}^{N \times S}$ $S \leq K = \text{rank}(P)$ represents the signal components. Noise and insignificant components are defined as $\Sigma_n \in \mathbb{R}^{M-S \times N-S}$, $U_n \in \mathbb{R}^{M \times M-S}$ $V_n \in \mathbb{R}^{N \times N-S}$.

To determine S , the ratio of the energy of signal components defined by singular values is calculated as

$$r_k \triangleq \frac{\sigma_k^2}{E_T}, \quad (39)$$

where E_T represents the total energy of scalogram matrix and σ_k^2 is the energy of k^{th} singular value. The singular values which are greater than the given threshold took place in the signal matrix

$\varepsilon (0 < \varepsilon \leq 1) ; r_1 \geq r_2 \geq \dots \geq r_s \geq \varepsilon \sum_s$. The rest of the K-S singular valued minor energy components are assumed to be noise. For signal components, scalogram matrix is obtained as $P_s = U_s \Sigma_s V_s^T$ where wavelet ridges are defined as the local maximum for every translation point (Özkurt, 2015).

The wavelet ridges of the noisy and less noisy brakes signals have been obtained and analyzed in the next chapter of this thesis.



2.5. Fourier versus Wavelet

Fourier Transform and Short Time Fourier Transform has been undoubtedly a pioneer tool in mathematics and science. Nevertheless, choosing an appropriate window size for satisfactory signal decomposition with STFT approach, is not guaranteed. The connatural uncertainty led most of the researchers to look for new approaches. The idea of Wavelet Transform has started to substitute for FT and STFT since the beginning of 1980's.

Wavelet Analysis has been a comprehensive and an extensive method with respect to FT and STFT thus preferred by scientists on numerous sorts of applications in the last three decades (Gao, 2011). The reason behind this is quite clear; wavelets are capable of using various and flexible windows while investigating the characteristics of a signal whereas classical methods like FT and STFT lack of, given in figure 2.18. It cuts up the data into different frequency components and works on every component with a resolution matching to its scale (Graps, 1995). The biggest advantage of wavelet transform compared to the old style methods is definitely the ability to keep the time information as well as frequency. This advantage offers an amending to resolution problem which STFT suffers. Also, short signal fragments have an importance in WT. Scaling (stretch) and shifting (delaying) for every instant is the main idea behind this tool, which allows the researcher to manipulate the data in a more revealing way.

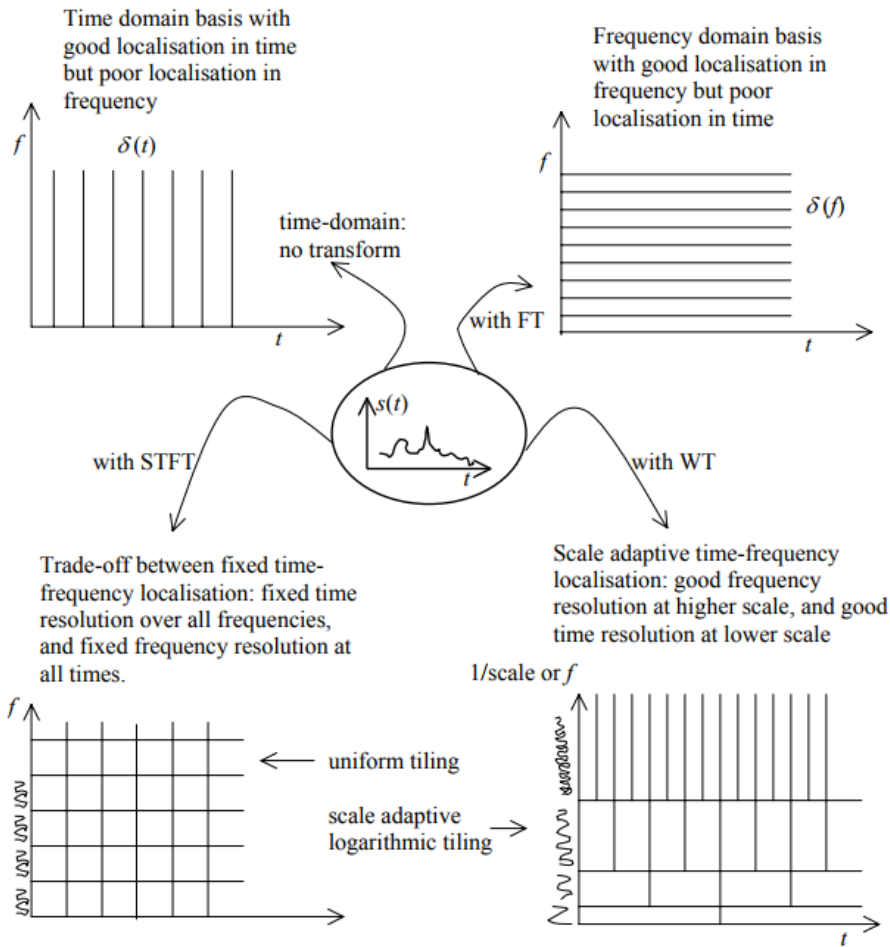


Figure 2.18. The comparison between FT, STFT and Wavelet Transform.

In the following chapter, the audio data collected at Ege Fren from a less noisy and noisy brake are investigated in time domain, frequency domain and time-frequency domain, respectively, regarding the theoretical information, summarized in this chapter.

CHAPTER 3

SOUND ACQUISITION AND ANALYSIS OF DISC BRAKE SYSTEM

Sound feature extraction and classification methods have been used by researchers frequently. The logic behind this application involves, extracting distinguishing features from the sound dataset and giving them into a classifier algorithm. Various approaches for different kind of sound features have been used in literature. Feature extraction from sound data, serves as the fundamental operation in the areas of signal processing, from health to security, mostly for malfunction detection and classification. Depending upon the choice of signal processing method, the features can be directly taken from time domain such as zero crossing rate, or from a transformation domain, such as Fourier Transform (FT), Mel-frequency cepstral coefficients (MFCCs). In transform domain, spectral similarity, entropy, octaves are some of the sound data features, with a great success rate (Umapathy, 2007). Some methods form a pattern from features in order to use it for classification. Another approach is to detect statistical parameters and feed them into a classifier. In this study, a noisy brake, a less noisy (wrt noisy one) and a noiseless (with no defect) has been compared in time domain, in frequency domain and in time-frequency domain respectively, in this study. This chapter covers, the data acquisition and analysis for aforementioned domains.

3.1. Data Acquisition

A Norsonic Type 1228 microphone has been located on the noisy disc brake with a proper setup. Then, by imc CRONOSflex data acquisition board given in figure 3.1, 150 seconds braking has been recorded for each type of brake while the driver pushes the brake pedal manually. The imc CRONOSflex 4 channel data acquisition board has a resolution of 16 bit and the sampling frequency is 20 kHz.

In 150 seconds record, braking instants for noisy, less noisy and noiseless brake; have been detected semi-automatically in Matlab by peak finder algorithm and inappropriate braking intervals are eliminated due to keep the data in the same 2 seconds pattern. Every braking instant and the following 2 seconds have been named as braking interval. Due to outer interferences and noises, some part of the data have been eliminated in order to keep the braking intervals same and safe. All in all, 39 braking intervals for less noisy brake and 30 braking intervals for noisy brake has been investigated in three different domains separately.

In engineering applications, normalization is performed to input data (audio for this case) as preprocessing in order to scale the signals in same level when analysis with respect to comparison is held. In this thesis, since all the data are collected in same environment and position of the microphones kept same, normalization hasn't been applied.



Figure 3.1. The imc CRONOSflex 4 channel data acquisition board

3.2. Time Domain Analysis

Discriminative features such as mean, variance, number of zero crossings, maximum, minimum, and entropy have been investigated in time domain for less noisy and noisy brakes.

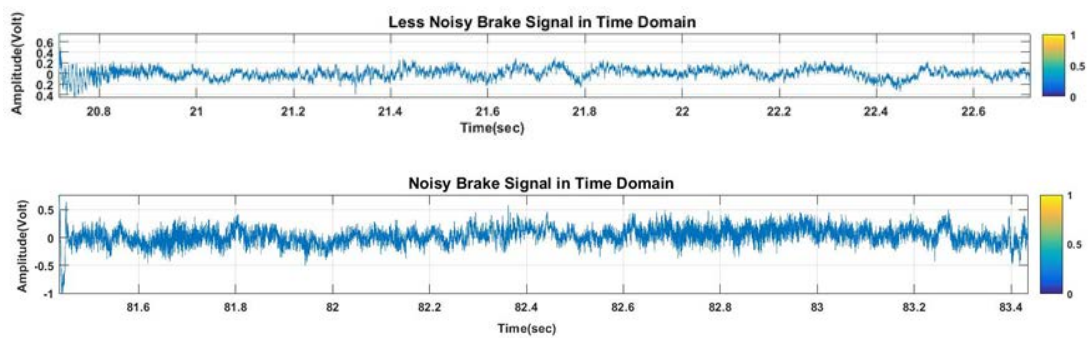


Figure 3.2. Two seconds braking interval representations of less noisy and noisy brake are shown in the figure above.

3.2.1. Mean

Mean or average refers to the central tendency of the elements in a dataset. In this study, for every braking interval (2 seconds fragment), the record of the signal has been obtained and the related mean is calculated by

$$M = \frac{1}{N} \sum_{n=0}^{N-1} x_n, \quad (40)$$

where M denotes the mean and N is the length of the signal and x_n is the braking interval. Average of this feature for all braking intervals of less noisy brake signals is -0.0013 in time domain.

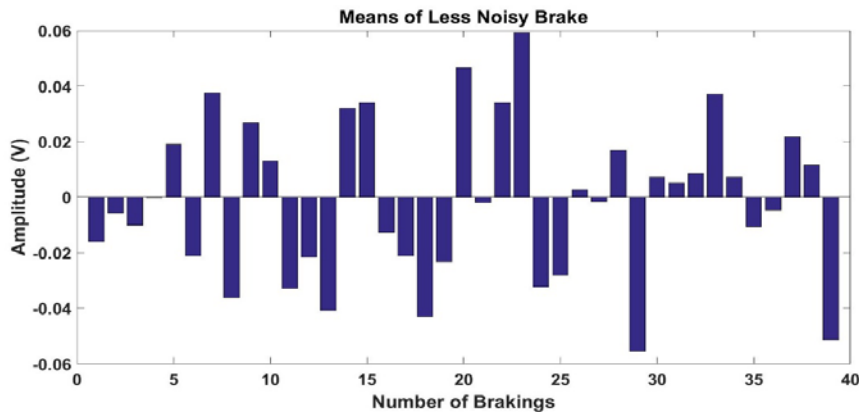


Figure 3.3. The mean of each braking interval in time domain for less noisy brake.

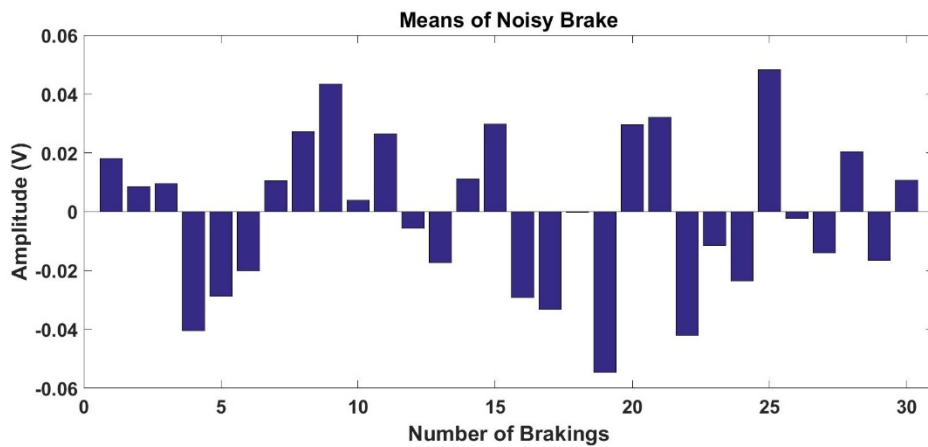


Figure 3.4. The mean of each braking interval in time domain for noisy brake.

Average of this feature for all braking intervals of noisy brake signals is -3.25×10^{-4} in time domain.

As can be observed from figure 3.3 and 3.4, the mean of same class of brake signals changes with every record and does not carry any knowledge about the signal class by itself.

3.2.2. Maximum

For every braking interval, maximum of the braking interval has been calculated by

$$A = \max(x_n), n = 0, 1, 2, \dots, N - 1, \quad (41)$$

where x_n denotes a braking interval and N is the number of brakings. Average of this feature for all braking intervals of less noisy brake signals is 0.57 in time domain.

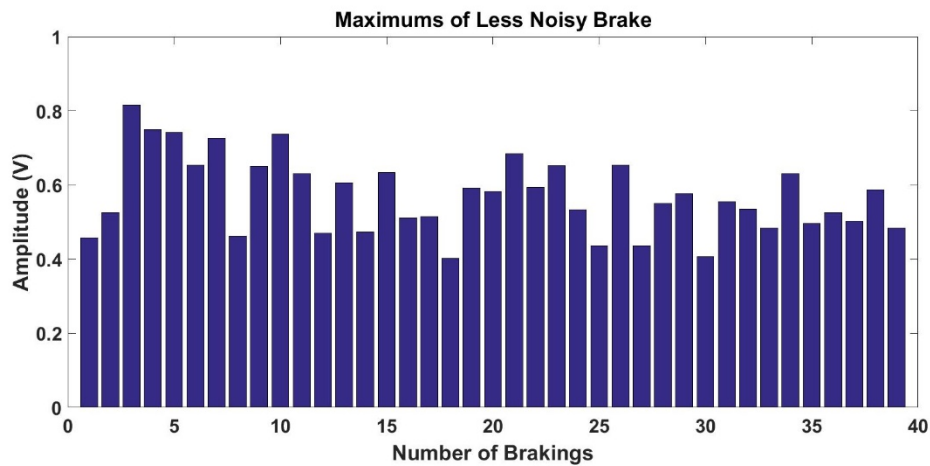


Figure 3.5. The maximum of each braking interval in time domain for less noisy brake.

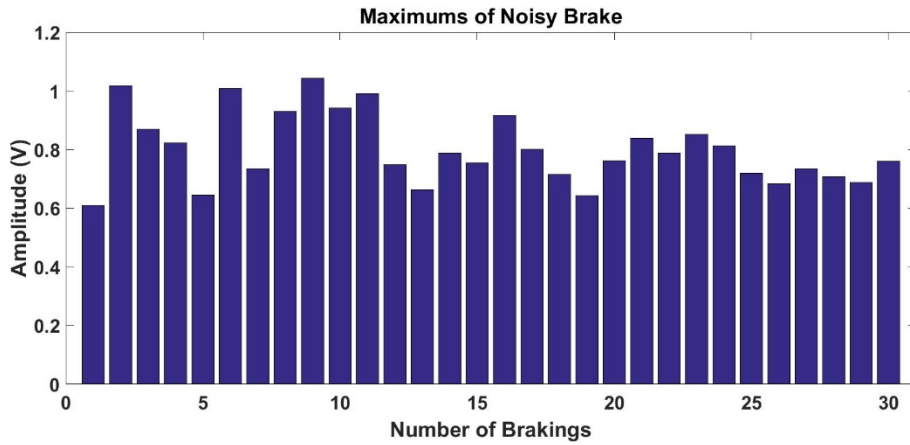


Figure 3.6. The maximum of each braking interval in time domain for noisy brake.

Average of this feature for all braking intervals of noisy brake signals is 0.79 in time domain.

As can be seen from figure 3.5 and 3.6, there is a slight difference between the averages of the maximums of each class.

3.2.3. Minimum

For every braking interval, minimum feature has been calculated by

$$A = \min(x_n), n = 0, 1, 2, \dots, N - 1, \quad (42)$$

where x_n denotes a braking interval and N is the number of brakings. Average of this feature for all braking intervals of less noisy brake signals is -0.46 in time domain.

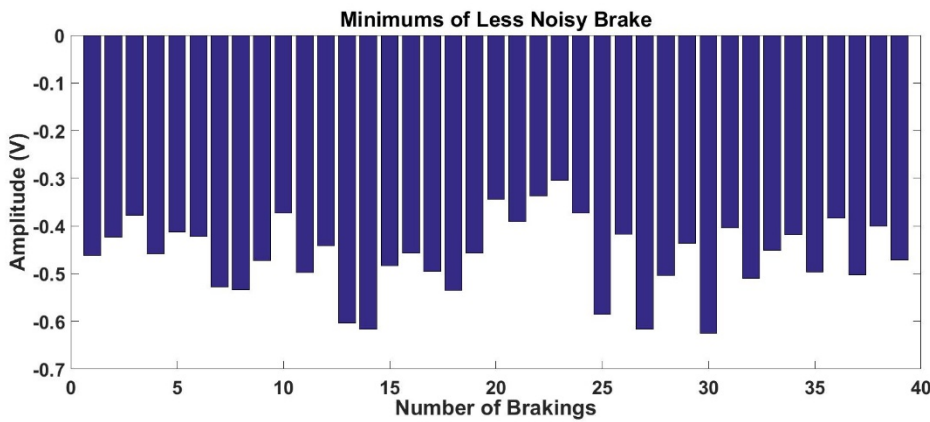


Figure 3.7. The minimum of each braking interval in time domain for less noisy brake.

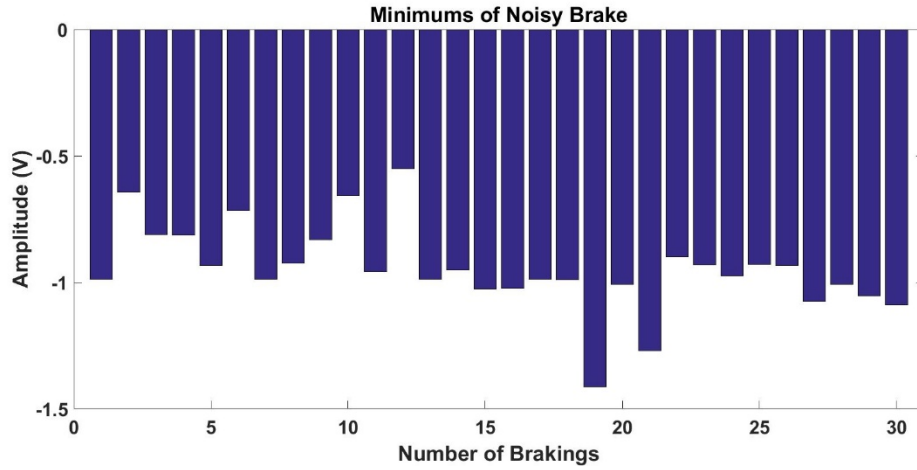


Figure 3.8. The minimum of each braking interval in time domain for noisy brake.

Average of this feature for all braking intervals of noisy brake signals is -0.94 in time domain.

As can be seen from figure 3.7 and 3.8, the minimums of each class shows some difference.

3.2.4. Variance

Variance is an informative statistical parameter that refers to the how any random variable is distributed with respect to mean value. Simply, it is defined as square of the standard deviation. For every braking interval (2 seconds fragment), the record of the signal has been obtained and the related variance is calculated by

$$V = \frac{1}{N-1} \sum_{n=1}^{N-1} (x_n - M)^2, \quad (43)$$

where M is the mean. Average of this feature for all braking intervals of less noisy brake signals is 0.0087 in time domain.

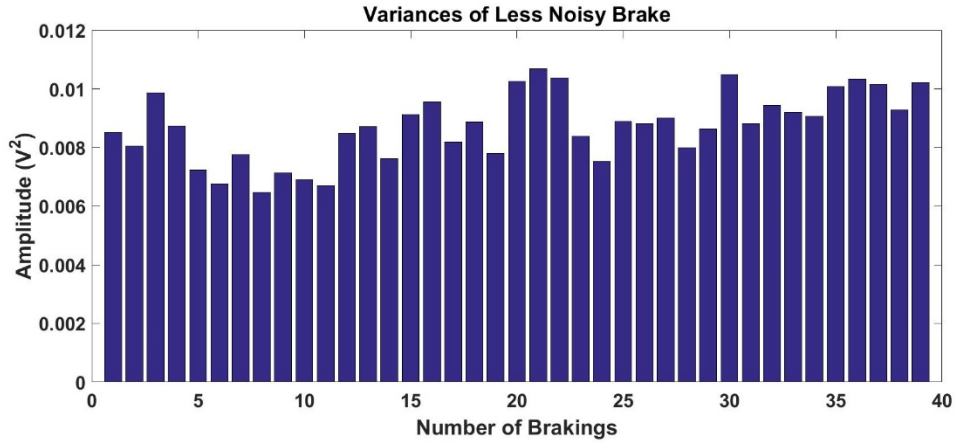


Figure 3.9. The variance of each braking interval in time domain for less noisy brake.

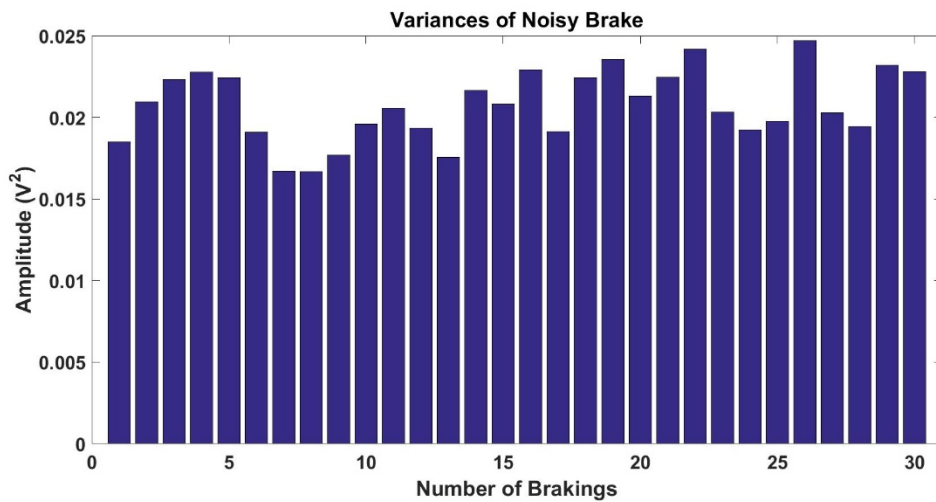


Figure 3.10. The variance of each braking interval in time domain for noisy brake.

Average of this feature for all braking intervals of noisy brake signals is 0.027 in time domain. Variance, refers to the square of standard deviation where it is shown to be more informative than standard deviation.

3.2.5. Number of Zero Crossings

Number of zero crossings refers to the dominant frequency in a signal spectrum. At first, for every braking interval (2 seconds fragment), the record of the signal has been obtained and the related number of zero crossings is calculated by

$$Z_t = \frac{1}{2} \sum_{n=1}^N |\text{sgn}(x[n]) - \text{sgn}(x[n-1])|, \quad (44)$$

where $x[n]$ denotes the n th element of the signal and N denotes the length signal (Schafer, 1975). Average of this feature for all braking intervals of less noisy brake signals is 3.4×10^3 in time domain.

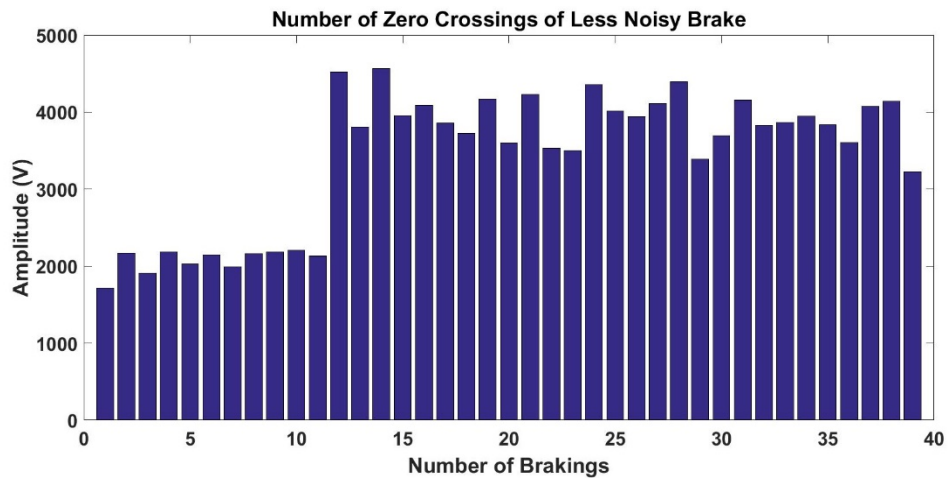


Figure 3.11. The number of zero crossings of each braking interval in time domain for less noisy brake.

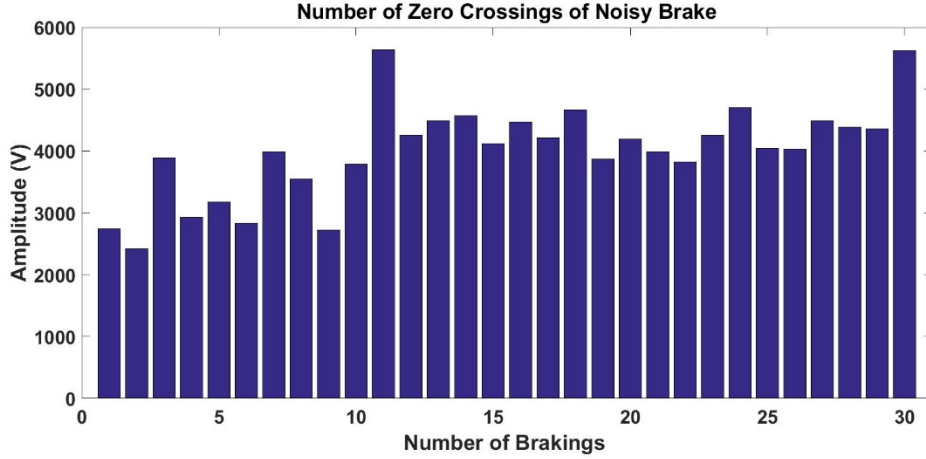


Figure 3.12. The number of zero crossings of each braking interval in time domain for noisy brake.

Average of this feature for all braking intervals of noisy brake signals is 4×10^3 in time domain.

In the records of less-noisy brakes given in figure 3.11, there is a considerable inter-class difference between the first 11 records and the remaining's. This difference has a negative effect on the features' discriminative abilities. It might be caused by the manual braking during record. The position of the driver's foot might have changed since the same characteristic is obtained in the following graphics.

3.2.6. Entropy

Entropy is a qualitative feature used to determine the complexity of a signal. In this study, for each braking interval time domain entropy is calculated as

$$\tilde{H} = - \sum_{k=0}^{L-1} n(x_k) \log_2 n(x_k), \quad (45)$$

where the relative frequency of the signal magnitude is $n(x_n) = \frac{n_k}{N}$ and n_k number of samples whose magnitude is in k^{th} bin in L levels. Average of included information is in terms of bits and this is why it has been represented by \log_2 .

Average of this feature for all braking intervals of less noisy brake signals is 1.90 in time domain.

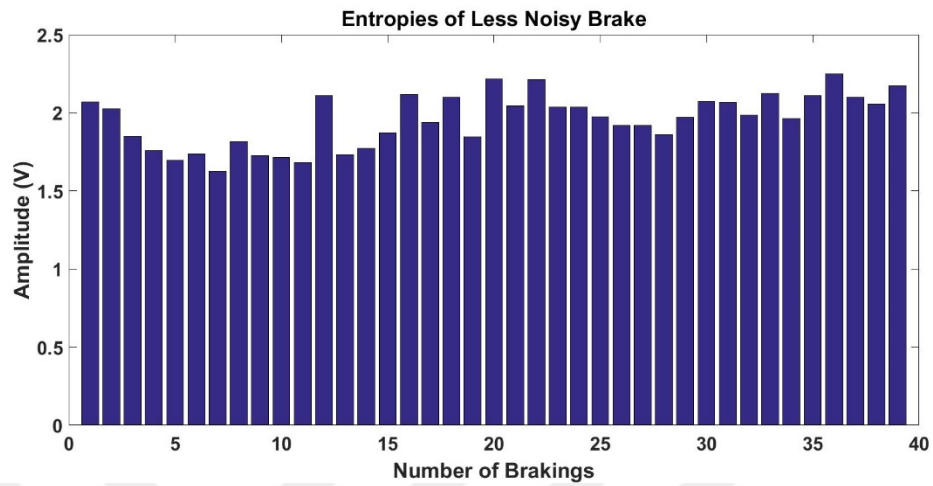


Figure 3.13. The entropy of each braking interval in time domain for less noisy brake.

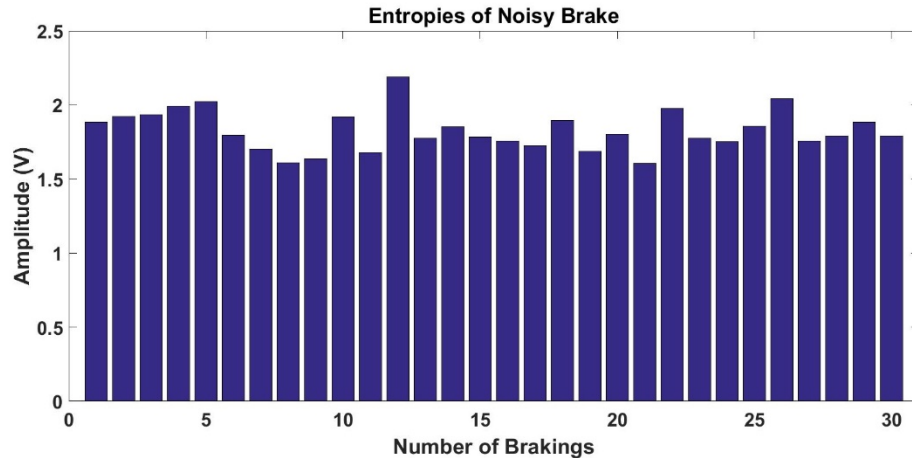


Figure 3.14. The entropy of each braking interval in time domain for noisy brake.

Average of this feature for all braking intervals of noisy brake signals is 1.82 in time domain. Feature entropy obviously, didn't show difference between two classes.

3.2.7. Classification Using Time Domain Features

In time domain classification, features of mean, variance, number of zero crossings, maximum, minimum and entropy are used as explained. For 39 less noisy and 30 noisy brake data, these features are computed in MATLAB then the outputs are fed into kth nearest neighbor classification algorithm.

K-Nearest Neighbors (k-NN) is one of the simplest machine learning method which classifies an input data by using its k nearest neighbors, widely used in pattern recognition. k-NN algorithm stores all possible cases and categorizes new cases based similarity. This method is applied as follows,

1. Choose K (number of nearest neighbor, $k=5$)
2. Evaluate the distance to other training data
3. Specify kth nearest neighbors
4. Use class labels of nearest neighbors to define the category of unknown data (similarity)

Similarity is defined as the distance between two points which could be Euclidean, Manhattan, Chebyshev and Hamming distances and are mostly used in pattern recognition.

K-NN is used when a labelled dataset consisting of training cluster (x,y) is given and needed to determine the relationship between x and y

$$P(y = j, X = x) = \frac{1}{K} \sum_{i \in A} I(y^i = j), \quad (46)$$

where x is the feature and y is the target. In order to keep predictive accuracy at highest, V- cross validation approach has been used due to the lack of the data. Cross validation basically states that, if there exists V folds, the first step of k-NN is to train the algorithm using $(V-1)$ of the folds, then test the accuracy of the algorithm where the first fold is neglected. This operation is repeated V times (for this study $V=10$) until each fold has been evaluated as in the test set.

When the success rate of classification has been computed for each feature individually, it is observed that minimum and variance statistical parameters gave the best results as shown in figure 3.16 where k=5, 10-fold cross validation is applied and the metric distance is calculated as City Block since it exhibited the highest accuracy among cosine, Chebyshev, hamming, spearman, correlation, Euclidean, Mahalanobis, Minkowski, Seucclidean and Jaccard.

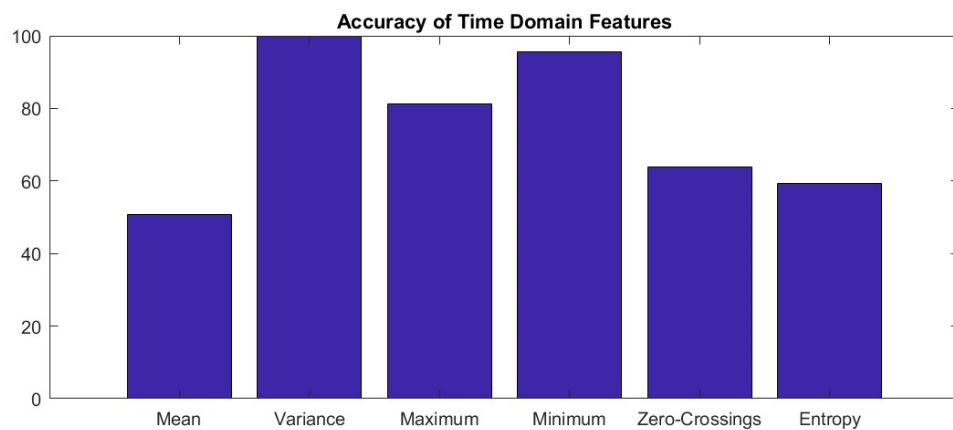


Figure 3.15. Accuracy of classification using time domain features.

Average of Time Domain Features		
	Less Noisy Brake	Noisy Brake
Maximum	0.57	0.79
Minimum	-0.46	-0.94
Mean	3.25×10^{-4}	-0.0013
Variance	0.0087	0.027
Number of Zero Crossings	3.4×10^3	4×10^3
Entropy	1.90	1.82

Table 3.1. Average values of features maximum, minimum, mean, variance, number of zero crossings and entropy for braking intervals of less noisy and noisy brake respectively.

As can be seen from Figure 3.15 and the table above, the features minimum and variance exhibited best results when they have been fed into k-NN classification algorithm, separately.

3.3. Frequency Domain Analysis

To have a complete analysis, the frequency domain features are also investigated. Discriminative features such as mean, variance, maximum, spectral roll-off, and entropy features have been investigated in frequency domain for less noisy and noisy brakes.

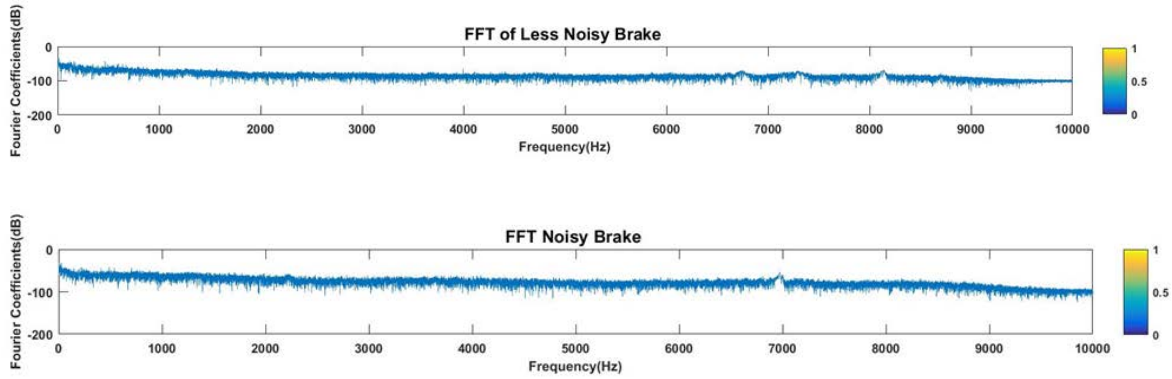


Figure 3.16. Two seconds braking interval representations of less noisy and noisy brake are shown in the figure above.

3.3.1. Mean of Frequency Distribution

Mean or average refers to the central tendency of the elements in a dataset. In this study, for every braking interval (2 seconds fragment), the FT of the signal has been obtained and the related mean is calculated by

$$M_f = \frac{1}{L} \sum_{k=0}^{L-1} X_k, \quad (47)$$

where M_f denotes the mean and L is the length of the signal and X_k is the FT. Average of this feature for all braking intervals of noisy brake signals is 6.12×10^{-4} in frequency domain.

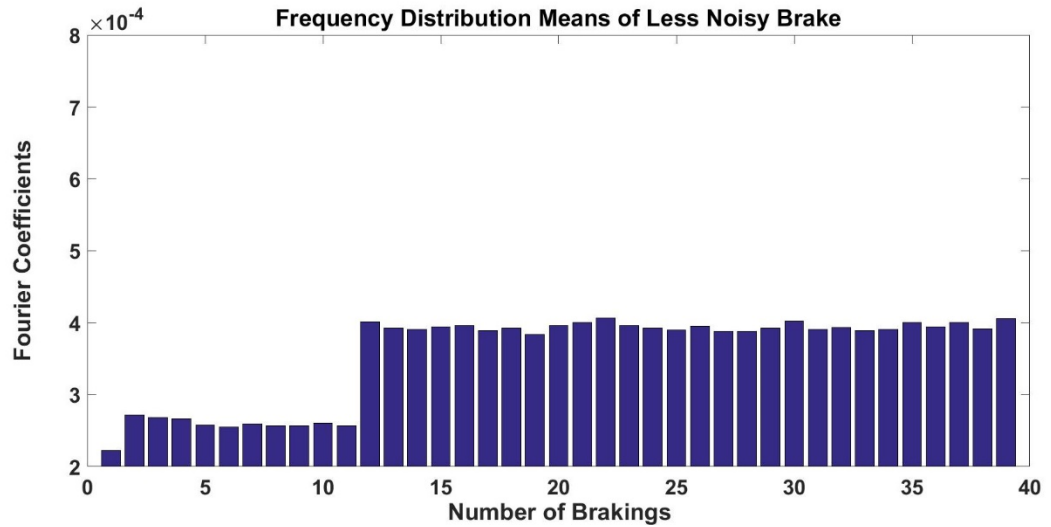


Figure 3.17. The mean of each braking interval in frequency domain for less noisy brake.

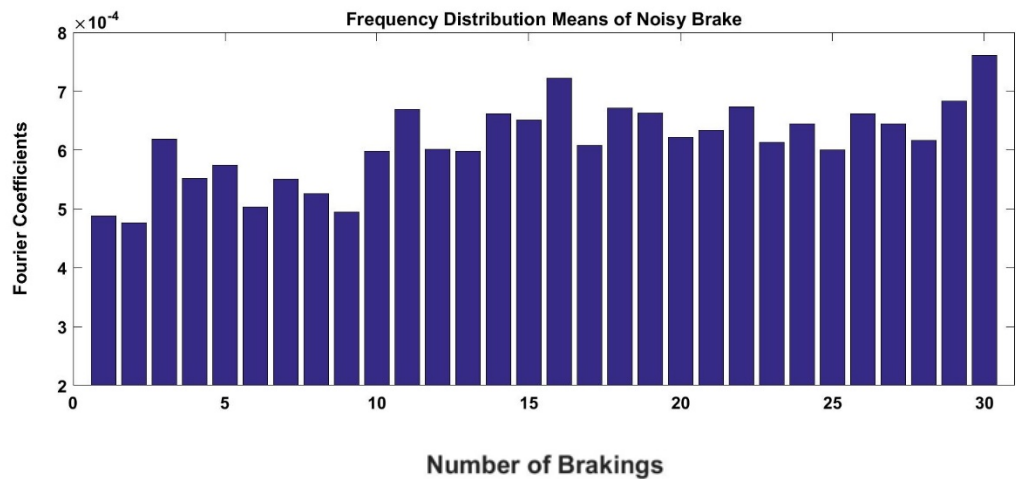


Figure 3.18. The mean of each braking interval in frequency domain for noisy brake. Average of this feature for all braking intervals of less noisy brake signals is 3.5×10^{-4} in frequency domain. There is a considerable difference regarding means of frequency distributions as can be seen above.

3.3.2. Variance

Variance is an informative statistical parameter that refers to the how any random variable is distributed with respect to mean value. Simply, it is the square of standard

deviation. After applying FFT to the every 2 seconds braking interval, variance is calculated by

$$V_{frequency} = \frac{1}{L-1} \sum_{k=1}^{L-1} (X_k - M_f)^2, \tag{48}$$

where M_f is the mean of frequency distribution. Average of this feature for all braking intervals of noisy brake signals is 1.8×10^{-6} in frequency domain.

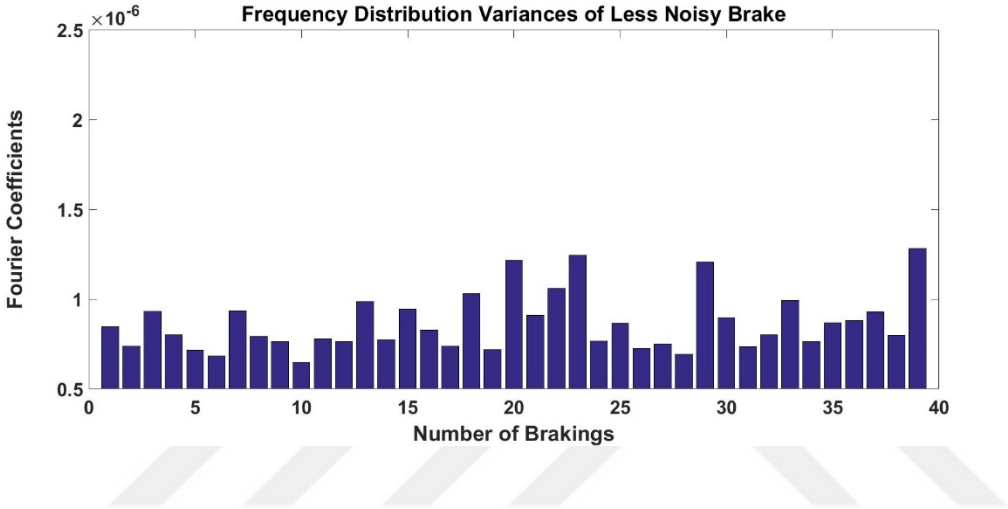


Figure 3.19. The variance of each braking interval in frequency domain for noisy brake.

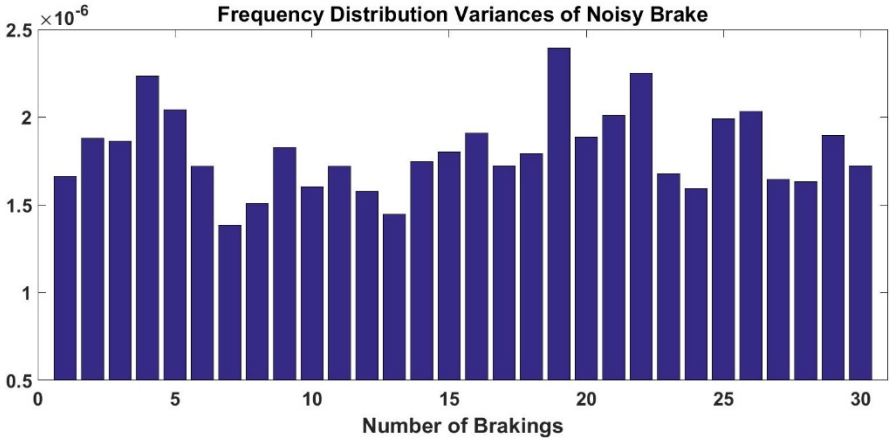


Figure 3.20. The variance of each braking interval in frequency domain for less noisy brake.

Average variance for all braking intervals of less noisy brake signals is 8.65×10^{-7} in frequency domain. A clear difference has been observed when the variance statistical parameter investigated in frequency domain.

3.3.3. Maximum

For every braking interval, maximum of the braking interval has been calculated by

$$A = \max(X_k), \quad k = 0, 1, 2, \dots, L - 1, \quad (49)$$

where X_k denotes maximum Fourier Coefficients of a braking interval and L is the number of frequency bins. Average of this feature for all braking intervals of less noisy brake signals is 0.0572 in frequency domain.

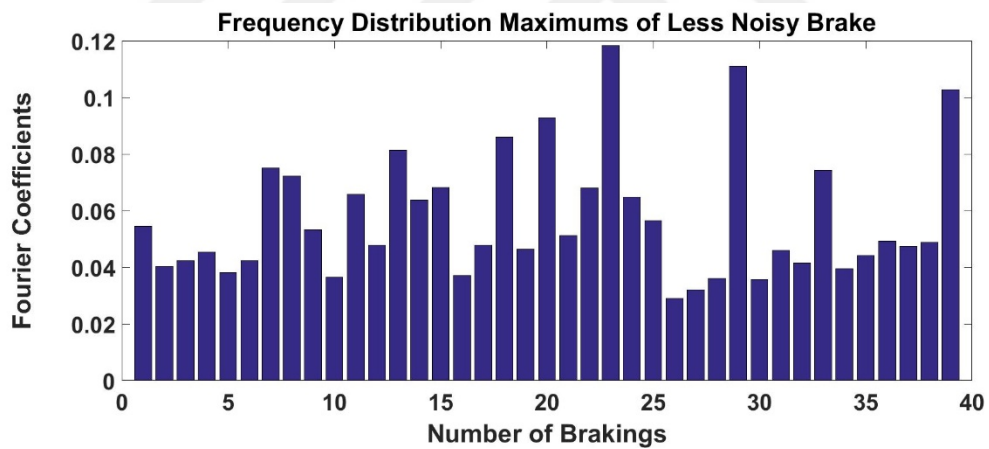


Figure 3.21. The maximum of each braking interval in frequency domain for less noisy brake.

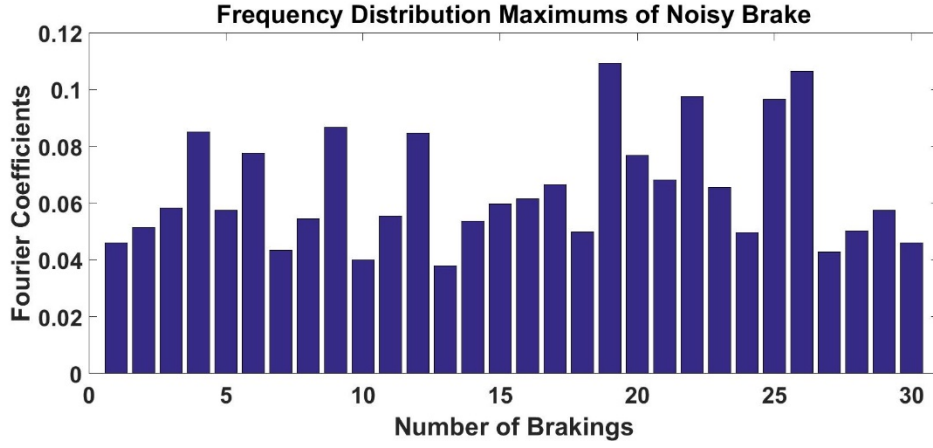


Figure 3.22. The maximum of each braking interval in frequency domain for noisy brake.

Average of this feature for all braking intervals of noisy brake signals is 0.0645 in frequency domain. Unfortunately this feature didn't show distinguishing characteristics in frequency domain.

3.3.4. Spectral Roll-off

Spectral roll-off point is a significant feature to determine the form of frequency spectrum. It is defined as R_k , which is the frequency where the 85 % of the magnitude distribution lies below,

$$Spectral\ Roll - off = \sum_{k=0}^{R_k} X_k^2 = 0.85 \sum_{k=0}^{L-1} X_k^2, \quad (50)$$

where X_k denotes the magnitude of k^{th} FT coefficient for 2 seconds braking interval. Since the less noisy brake has less complex signal components, the spectral roll-off feature is greater than noisy one, as expected. Average of this feature for all braking intervals of noisy brake signals is 4922.74 in frequency domain.

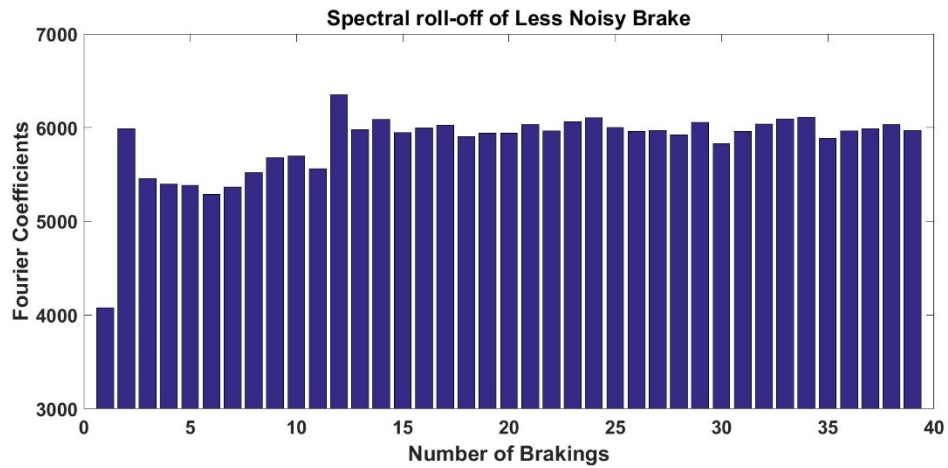


Figure 3.23. The spectral roll-off of each braking interval in frequency domain for noisy brake.

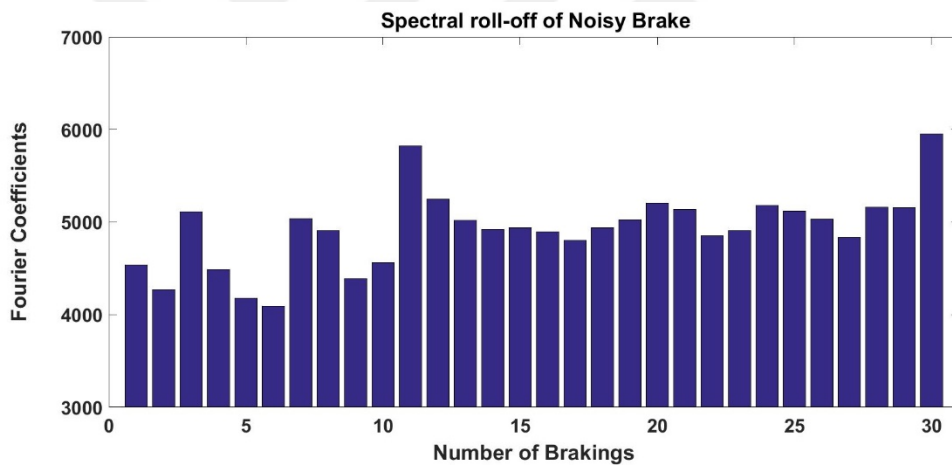


Figure 3.24. The spectral roll-off of each braking interval in frequency domain for less noisy brake.

Average of this feature for all braking intervals of less noisy brake signals is 5833.86 in frequency domain. Spectral roll-off feature might be an informing tool while investigating the differences between less noisy and noisy brake as can be seen in the figures above.

3.3.5. Entropy

Entropy is a qualitative feature used to determine the complexity of a signal. In this study, regarding the $n(X_k)$ as relative frequency value of FT for each braking interval entropy is calculated by

$$\tilde{H} = - \sum_{k=0}^{L-1} n(X_k) \log_2 n(X_k) , \quad (51)$$

Average of included information is in terms of bits (Duda, 2012) and this is why it has been represented by \log_2 .

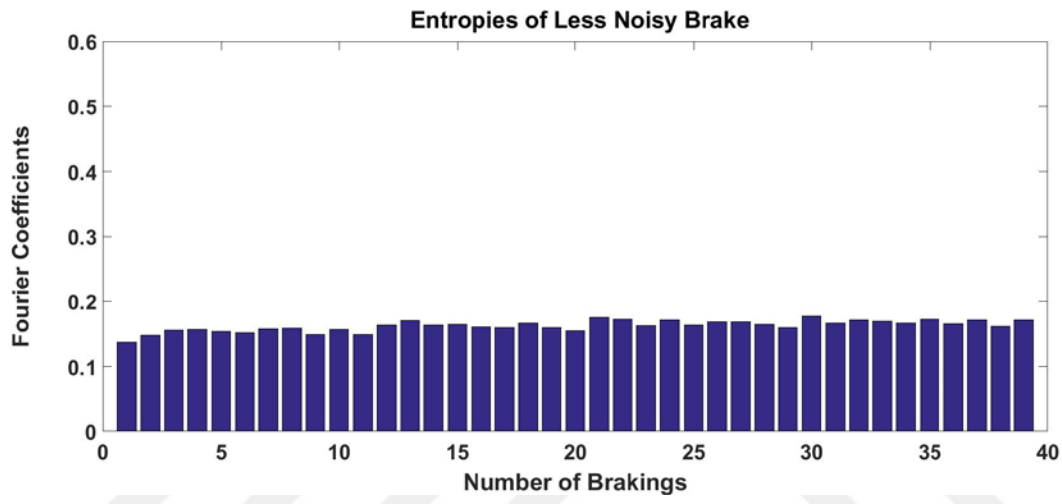


Figure 3.25. Entropy of each braking interval in frequency domain for noisy brake.

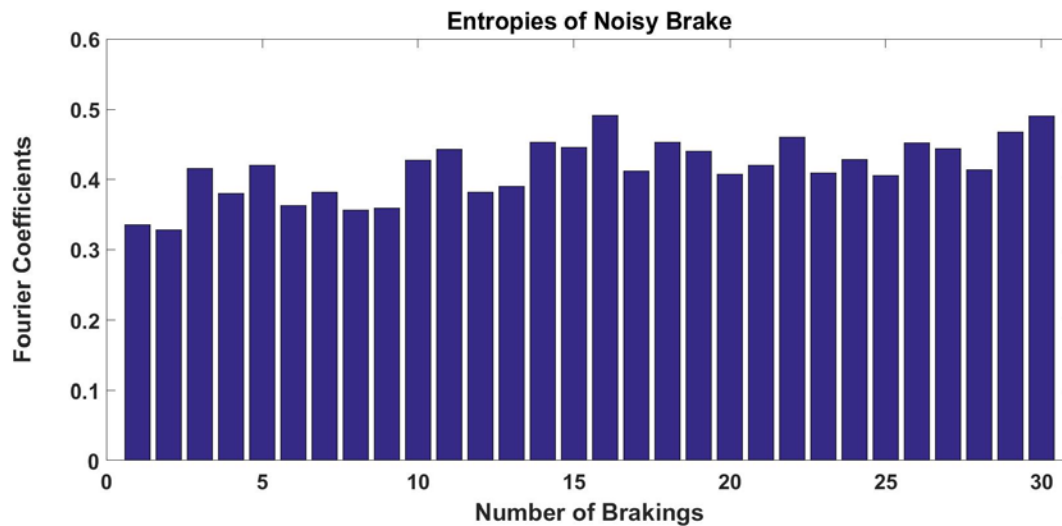


Figure 3.26. Entropy of each braking interval in frequency domain for less noisy brake.

Average entropies of noisy brake signals is 0.41 while average entropies of less noisy brake signals is 0.16 in frequency domain. As expected, the noisy brake signals have more complex frequency domain pattern, therefore the entropy values are higher.

3.3.6. Classification with Frequency Domain Features

In frequency domain features mean, spectral roll-off, variance, maximum and entropy has been investigated for less noisy and noisy brake. Features entropy, spectral roll-off variance and mean have given the best results whereas maximum feature failed respectively.

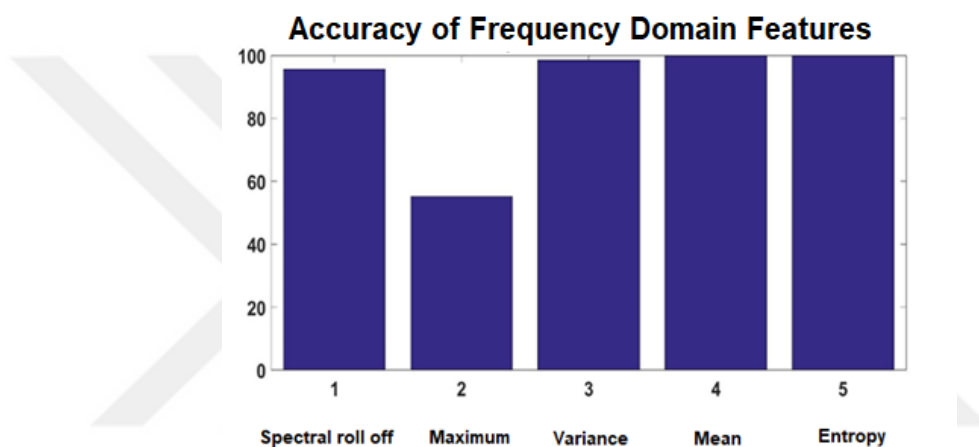


Figure 3.27. Spectral roll-off, maximum, variance, mean and entropy features classification accuracy is shown.

Average of Frequency Domain Features		
	Less Noisy Brake	Noisy Brake
Maximum	0.0572	0.0645
Mean	3.5×10^{-4}	6.12×10^{-4}
Variance	8.65×10^{-7}	1.8×10^{-6}
Spectral roll-off	4922.74	5833.86
Entropy	0.16	0.41

Table 3.2. Average values of features maximum, minimum, mean, variance, number of zero crossings and entropy for braking intervals of less noisy and noisy brake respectively.

As can be seen from Figure 3.27 and the table above, the features mean, entropy and variance exhibited best results when they have been fed into k-NN classification algorithm, separately.

3.4. Time-Frequency Domain Analysis Using Complex Wavelet

To improve the analysis, qualitative and quantitative analysis in time-frequency domain has been accomplished using wavelet analysis. The complex morlet wavelet has been used since,

1. It has a different frequency modulation
2. It is easy to modify both the amplitude and the phase of coefficients.

The complex wavelet transform has been applied on the data; 30 braking interval for noisy brake, 39 braking interval for less noisy brake and 11 braking interval for noiseless brake. Heuristically, it has been observed that cmor1-10 wavelet whose center frequency is 10 Hz and bandwidth is 1Hz has given a good resolution in time-frequency domain as shown in Figure 3.32, 3.33 and 3.34 respectively. The analysis has been performed in 400Hz – 2 kHz range which encompasses most of the signal energy. Noise threshold has been chosen as $\epsilon=0.01$ namely, signal components whose energy contribution was more than 1 % have been used. In figure 3.4 and 3.7 it is clear that, there are far more signal components in noisy brake with respect to less noisy brake's energy distribution.

In Figure 3.33 and 3.34, dark blue color wavelet ridge shows where the signal has no energy whereas light blues and yellows represents a higher signal intensity. For all type of brakes, low frequency signal components have been observed during all braking intervals in the range of 1 kHz. However, in the range of 1-2 kHz, very intense signal components have been observed during the analysis of noisy brake. For noiseless brake, almost no wavelet ridges have been obtained except braking instant and air evacuation (depletion).

For all braking intervals, the qualitative same pattern has been observed in Matlab analysis. In order to evaluate the braking intervals also quantitatively, the wavelet ridge matrix have been considered as an image and entropy of the image has been calculated.

In a digital image the probability of intensity or probability of gray level occurrence has been defined as,

$$p_r(r_k) = \frac{n_k}{MN} \quad k = 0, 1, 2, \dots, L - 1, \quad (52)$$

Where MN denotes the total number of pixels in the image, n_k represents the number of pixels which have intensity of (r_k) and L shows the probable intensity levels. By using $p_r(r_k)$ entropy can be calculated.

$$\tilde{H} = - \sum_{k=0}^{L-1} p_r(r_k) \log_2 p_r(r_k), \quad (53)$$

Average of included information is in terms of bits and this is why it has been represented by \log_2 . By assuming wavelet ridge matrices as image matrices, entropy has been calculated for every brake signal for each type of brake separately. Matlab outputs have supported the observations as well.

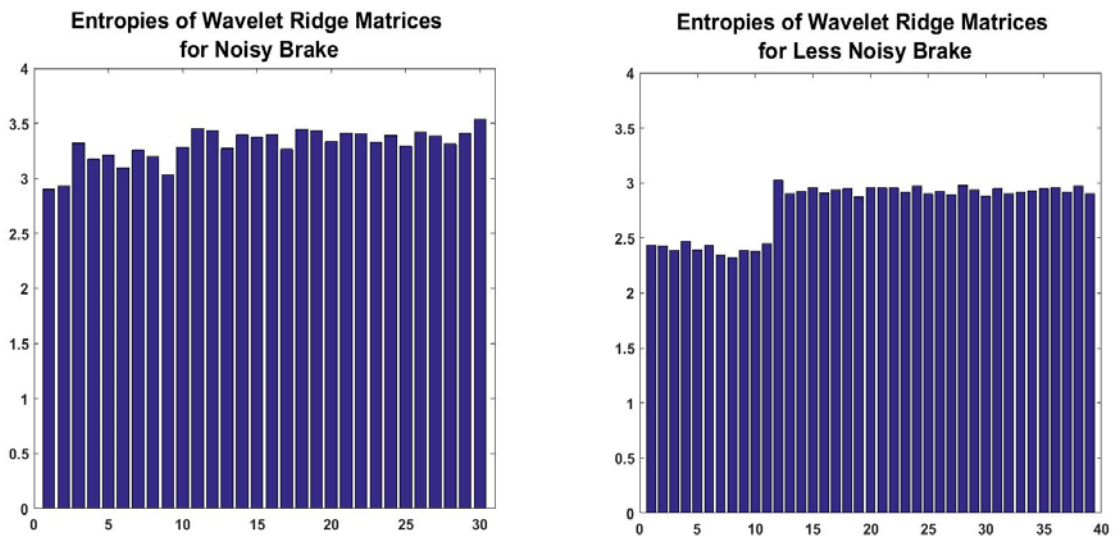


Figure 3.28. Comparison of entropy of wavelet ridge images for less noisy and noisy brakes.

Heuristically, cmor1-20 wavelet, which has the same center frequency with the previous wavelet but has a bandwidth of 20 Hz, has been chosen as a window function, and the difference was obvious. This complex wavelet clearly performed a higher resolution for noise data acquired from brakes. Given in Figure 3.29 and Figure 3.32, cmor1-10 vs cmor1-20 wavelet analysis for a noiseless air disc brake has been given. Obviously, only the air evacuation is seen whereas in figure 3.30 and figure 3.33 less noisy brakes are investigated using cmor1-10 and cmor1-20 respectively. The same wavelets are again applied on to noisy brake data where the noise components are detected clearly.



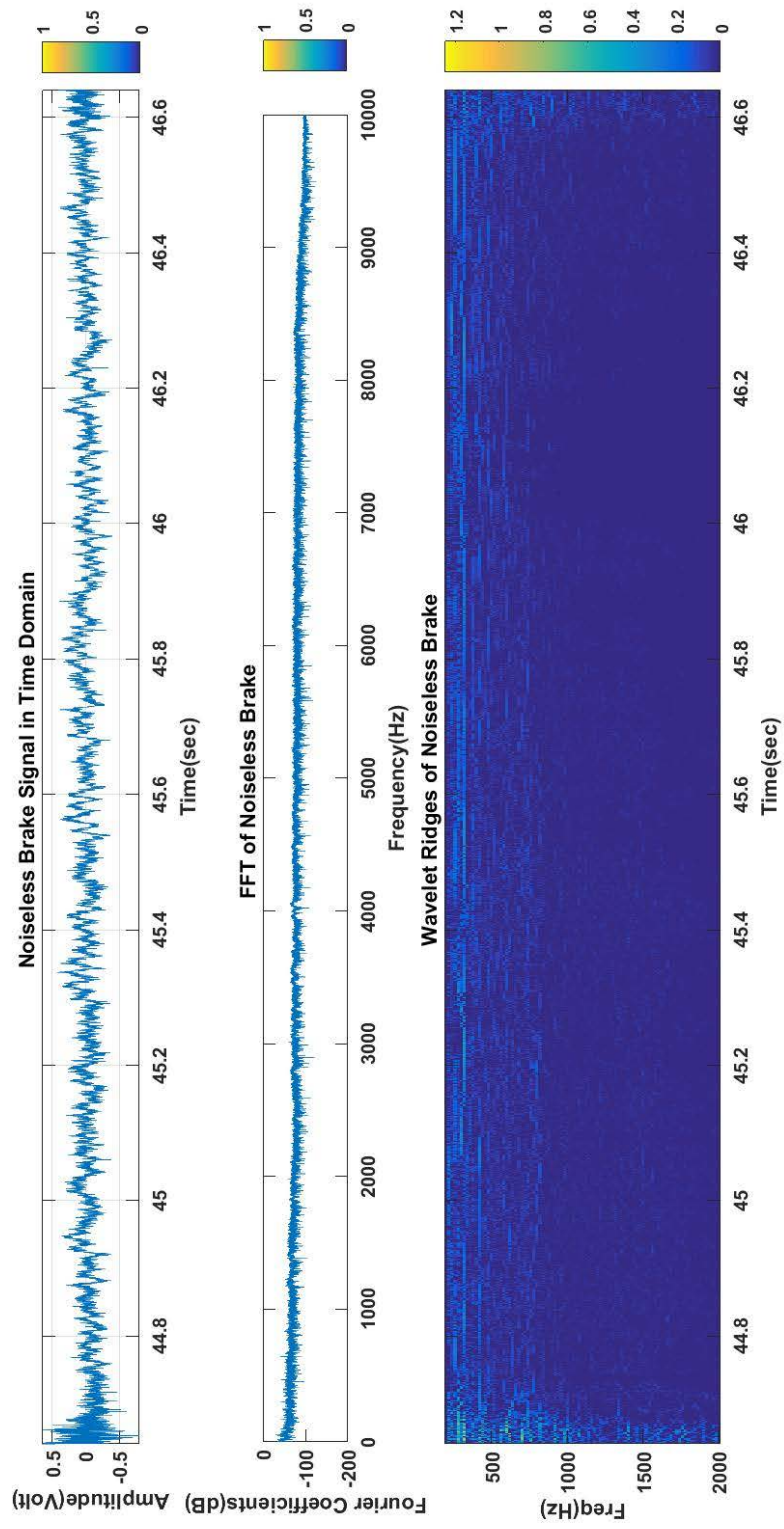


Figure 3.29. Time domain, frequency domain and time-frequency domain representations of a noiseless brake, using cmor 1-20 wavelet.

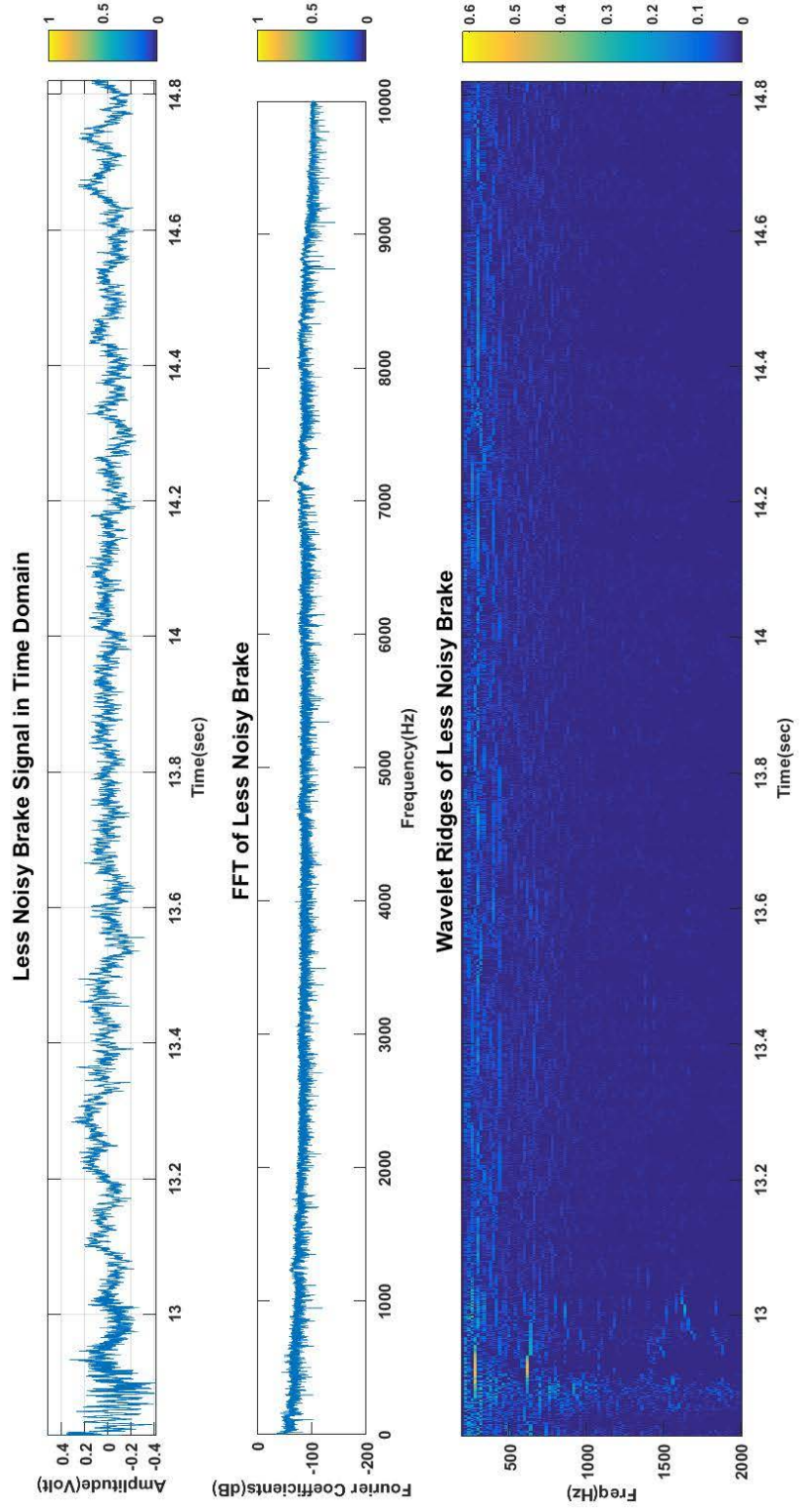


Figure 3.30. Time domain, frequency domain and time-frequency domain representations of less noisy brake, using cmor 1-20 wavelet.

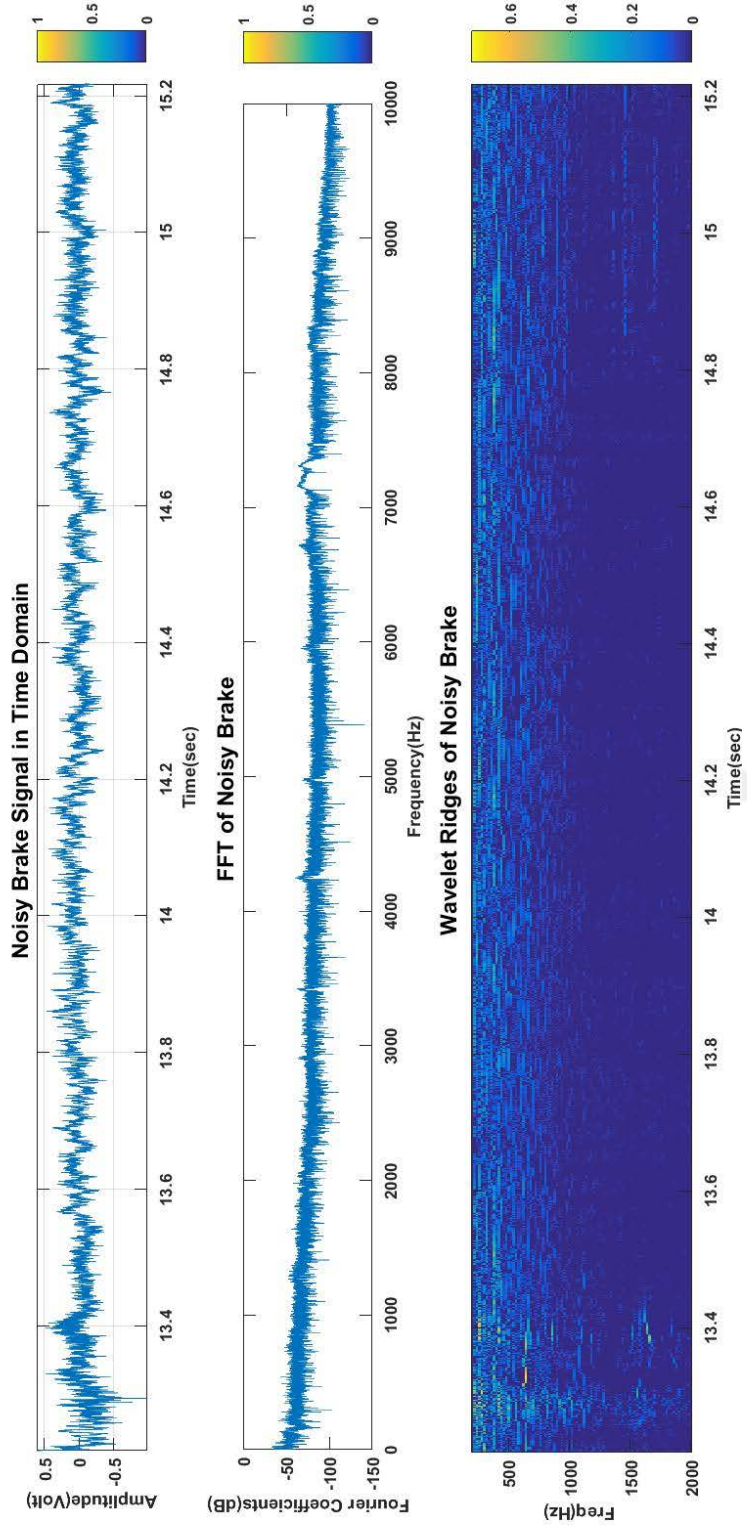


Figure 3.31. Time domain, frequency domain and time-frequency domain representations of a noisy brake, using cmor 1-20 wavelet.

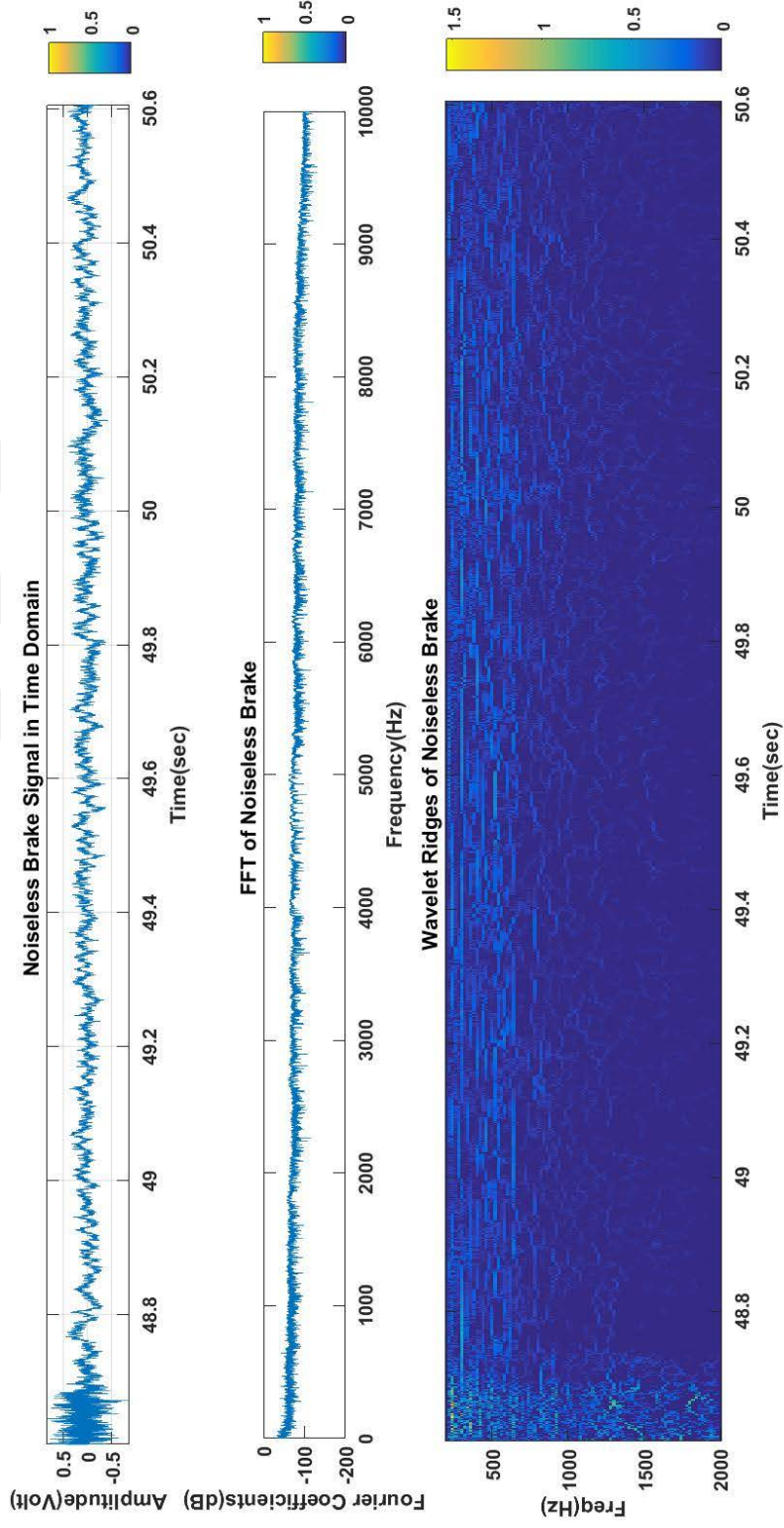


Figure 3.32. Time domain, frequency domain and time-frequency domain representations of a noiseless brake, using cmor 1-10 wavelet.

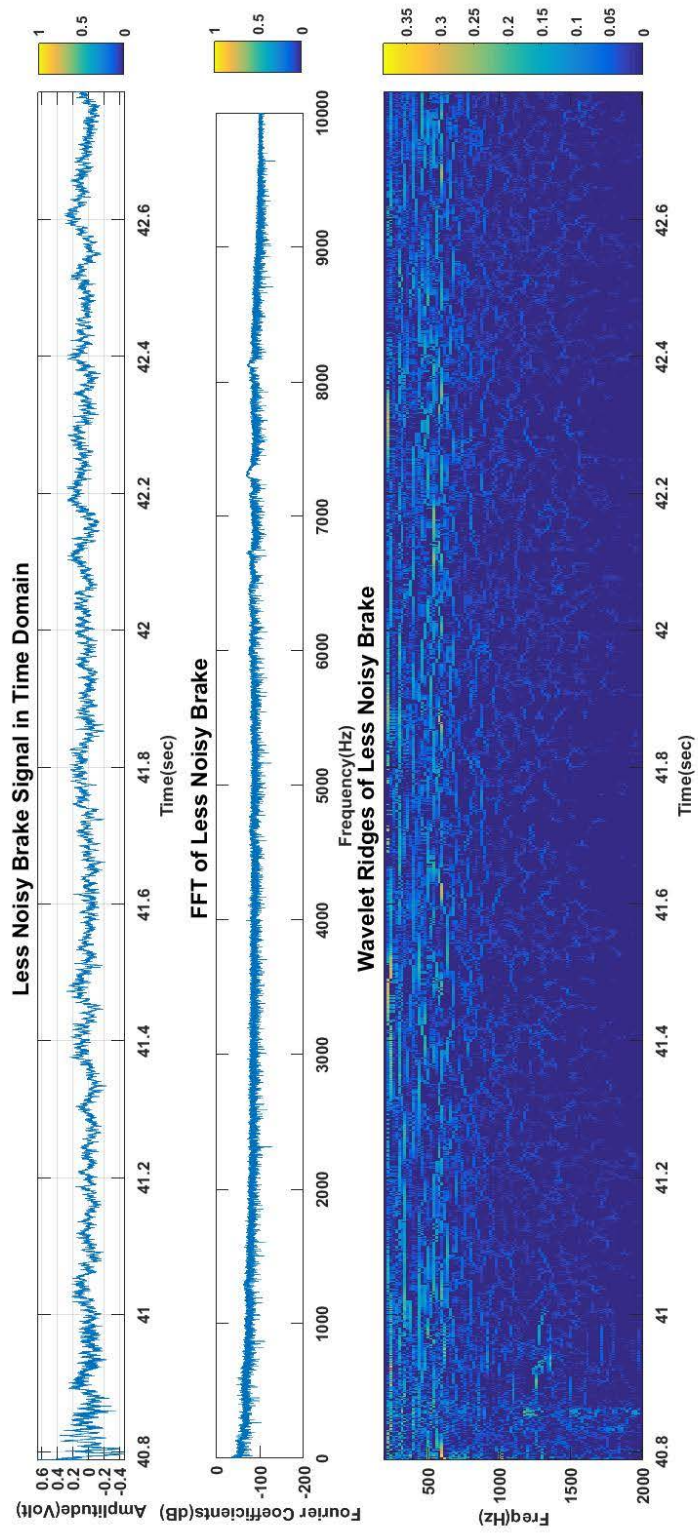


Figure 3.33. Time domain, frequency domain and time-frequency domain representations of a less noisy brake, using cmor 1-10 wavelet.

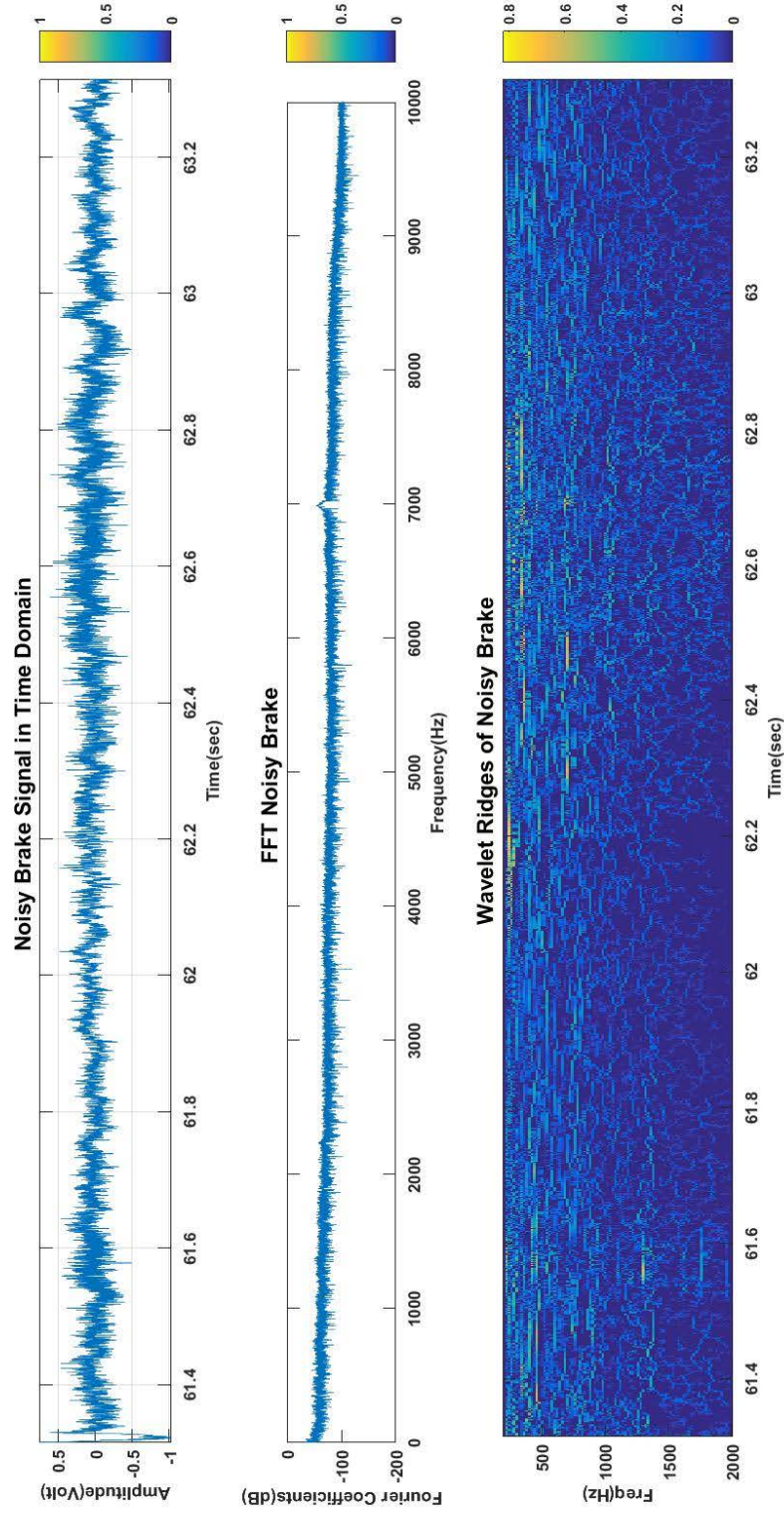


Figure 3.34. Time domain, frequency domain and time-frequency domain representations of a noisy brake, using cmor 1-10 wavelet.

3.5. Time-frequency Domain Classification Using DWT

In this section, the brake signals are classified into two groups by using statistical parameters of DWT coefficients. The block diagram of the applied algorithm is shown in Figure 3.35. As given in chapter 2.3 Daubechies wavelets Db3, Db6, Db9, Db10, Db12, Db15 and Db18 have been chosen as mother wavelets. After DWT has been applied for 10 levels of noisy (30) and less noisy (39) brake data; mean, standard deviation, energy and entropy features has been computed. These statistical parameters have been given into k-NN algorithm.

In this part of the study, 10-fold cross validation k-NN algorithm has been used in order to classify brakes as noisy or less noisy. 8 types of Daubechies wavelet has been used for classification, considering 4 main features.

The calculated features for db3, db6, db9, db10, db12, db15 and db18 wavelets are given into classification algorithm and success rates are given in figure 3.36.

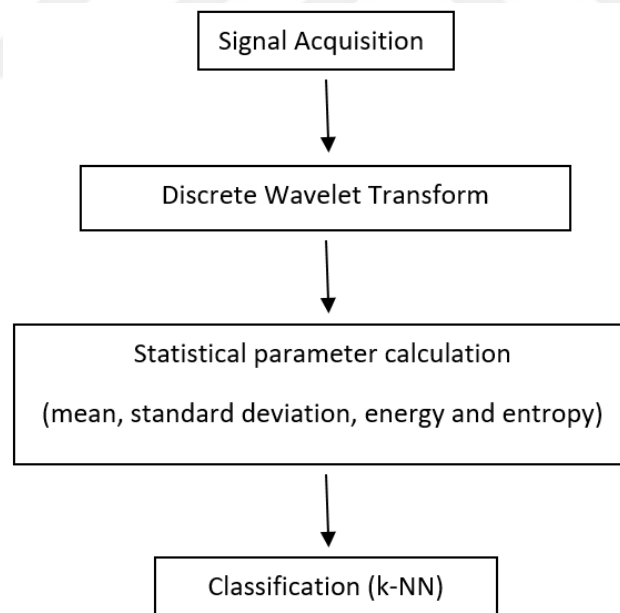


Figure 3.35. Process of brake classification using DWT

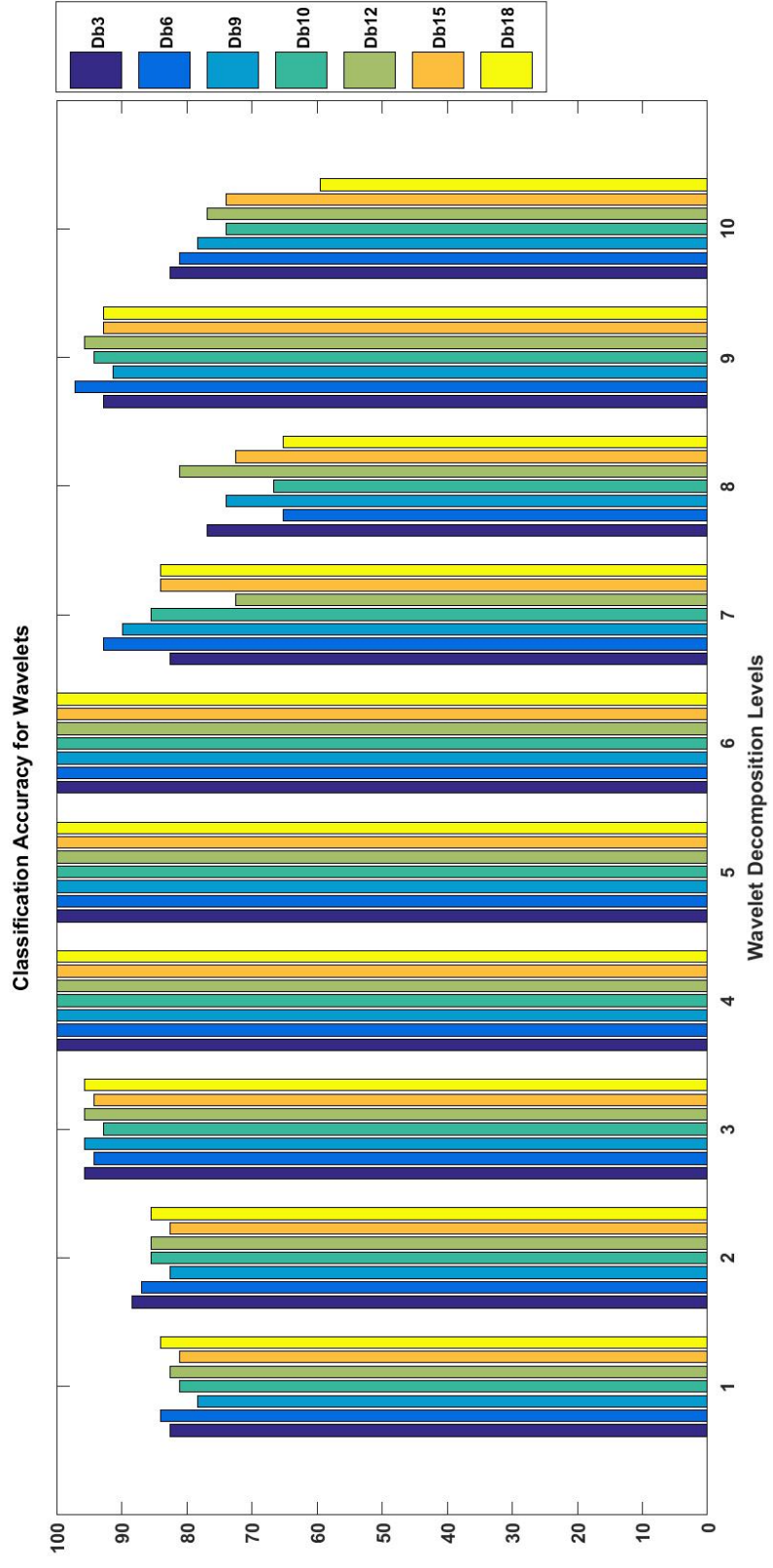


Figure 3.36. Classification accuracy for different order of Daubechies wavelet family

In figure 3.36, classification accuracy of noisy and less noisy brakes are given. It is obvious that, for level 4, 5 and 6; all the derivatives of Daubechies wavelets (db3, db6, db9, db10, db12, db15 and db18) gave 100 % success rate when fed into k-NN classification algorithm.

CHAPTER 4

CONCLUSIONS AND FUTURE RESEARCH

Sound and noise processing is a very promising technique as they have been referred in the introduction chapter. Researchers use this approach mostly in order to detect and classify disorders. Sometimes it is useful to follow up periodic movements or radical differences in a dataset. Many practical applications of noise processing can be found in the literature, from economy & finance to biomedical signal processing. Also in image processing, wavelet transform is a pioneering tool due it's one of the biggest advantage, higher resolution.

Since the FT has been proposed and approved in 1800s, it also triggered an innovative perspective for scientists. Frequency components of a signal has been informative for signal processing since it has been put forward but there had been one thing missing. At what time exactly, did that particular frequency component form? This question had led another approach, STFT, which provided time information with a limited resolution quality due to the uncertainty principle. At the end of 1990s wavelet theory has been put forward and developed immediately. After industrial revolution, manufacturing machines and processes became more and more complex and this entailed safer and cheaper operation with higher quality. Midproducts, final products and the processes as well are continuously monitored, and delays or faults are evaluated. This is realized by using the signals collected via sensors like temperature, noise, pressure, gas detector etc.. These signals are mostly in time domain and in order to pull out discriminative information and bring out characteristics of such signals, an adequate signal processing method has been proposed, Wavelet Transformation. It has been widely used since late 1990's, the applications are carried out in numerous areas where WT keeps developing itself day by day.

Lately, fault or disorder detection and classification using wavelet functions' advantages is a fairly used approach. In this thesis, sound signals collected from

noiseless, less noisy and noisy brakes have been investigated in time domain, in frequency domain and in time-frequency domain respectively.

In time domain, the raw data has been cut up into braking intervals and at the end of data acquisition, 39 braking intervals for less noisy and 30 braking intervals for noisy brake has been obtained. These intervals have been extracted semi automatically using peak finder algorithm. Statistical parameters have been searched in time domain and results have been given into k-NN classification algorithm. It has been observed that the variance and minimum has produced best results.

A very well-known approach in frequency domain analysis, FFT has been applied to these signals and again features in frequency domain have been given into classification algorithm and immensely promising results have been obtained. For a higher resolution signal spectrum, wavelet transform of these data have been practiced. Firstly, complex wavelet transformation has been realized for noisy and less noisy brakes. For every braking interval, using cmor1-10 wavelet, entropies of digital images have been calculated and compared in Matlab. The qualitative feature entropy has been observed as a distinguishing feature. The mean of less noisy brakes' was calculated as 2.78 and standard deviation 0.24 whereas mean of noisy brakes' was 3.30 and standard deviation was 0.15 respectively. Same study has been applied once more using cmor1-20 wavelet, and the results were not far more different as, mean of less noisy brakes' was 2.48 and standard deviation was 0.3695 whereas mean of noisy brakes' was 2.86 and standard deviation was 0.23 respectively.

Finally a more compact analysis has been performed, the DWT. According to this method, the detail and approximation coefficients of the signals has been obtained by successive applications of high and low pass filters. This led us to implement discrete wavelet transform for 10 levels and the outputs again have been fed into k- nearest neighborhood algorithm. Derivatives of Daubechies wavelet have been compared. The best success rate has been observed in Daubechies3 wavelet for level 4, 5 and 6 and gave us hope to improve semi-automatic or automatic systems to detect faults or disorders.

The classification rates up to 100% have been obtained for different features from time, frequency and time-frequency domain. However, the number of the measurements

were not adequate for making certain conclusions about the selection of features. In spite of the fact of insufficient data, the study covered all aspects of the analysis for a fault analysis system.

In the thriving automobile industry, determining the root cause of a problem and repair of a vehicle unfortunately takes time, work labor and money. Due to the disadvantages of manual intervention and diagnosis, fault analysis from noise and vibration data has been more important than ever which encourages researchers to study on.

One of the biggest trouble encountered in data acquisition process is, noise and vibration signals are so tender that, any outsider triggering factor between two pedaling moments, can impact the purity. Another challenge I observed during this study is, due to the nature of air disc brakes, we hear an air evacuation noise as expected. The problem is, during data acquisition; there must be enough time elapsed that let the sound residuals from the previous braking fade away. Inadequate attenuation of noise signals may have a negative effect on the discriminative characteristics of the features. This precaution is so significant to obtain clear data.

In addition, one of the biggest difficulty we have confronted during this study is, lack of open access data sets. For the sake of development in signal processing, scientists must be able to perform different analysis methods compare them to argue on different approaches.

REFERENCES

- Addison, P. S. (2017). *The illustrated wavelet transform handbook: introductory theory and applications in science, engineering, medicine and finance*. CRC press.
- Communications Applications Conference (SIU), 2018 26th. IEEE.
- Dalgacık Tepeleri Yöntemi ile Ses Analizi. In *Çukurova University Journal of the Department of Radio Engineering K13137*, CTU FEE, Prague (2018), Wavelet Toolbox, Daubechies http://radio.feld.cvut.cz/matlab/toolbox/wavelet/ch01_31a.html
- Duda, R. O., Hart, P. E., & Stork, D. G. (2012). *Pattern classification*. John Wiley & Sons.
- Dunlap, K. B., Riehle, M. A., & Longhouse, R. E. (1999). *An investigative overview of automotive disc brake noise* (No. 1999-01-0142). SAE Technical Paper.
- Ertekin, Z., & Özkurt, N. (2018, May). Analysis and Classification of Air Disc Brake
- Ertekin, Z., Özkurt, N., & Yilmaz, C. (2017, December). Disk Fren Sistemlerinde *Faculty of Engineering and Architecture*, 32(4), 193-200.
- Gajre, M. N., Jegadeeshwaran, R., Sugumaran, V., & Talbar, A. (2016). Vibration based fault diagnosis of automobile hydraulic brake system using fuzzy logic with best first tree rules. *International Journal of Vehicle Structures & Systems*, 8(4), 214.
- Gao, R. X., & Yan, R. (2011). From Fourier transform to wavelet transform: a historical perspective. In *Wavelets* (pp. 17-32). Springer, Boston, MA.
- George Dallas (2016), Signal Processing, Fourier Transforms and Heisenberg UK based Information Engineer/ Internet Social Scientist <https://georgemdallas.wordpress.com/2014/05/14/wavelets-4-dummies-signal-processing-fourier-transforms-and-heisenberg/>
- Ghazaly, N. M., El-Sharkawy, M., & Ahmed, I. (2014). A review of automotive brake squeal mechanisms. *J Mech Des Vib*, 1(1), 5-9.

- Graps, A. (1995). An introduction to wavelets. *IEEE computational science and engineering*, 2(2), 50-61.
- Halderman, J. D., & Mitchell, C. D. (1996). *Automotive brake systems*. Prentice Hall.
- Haykin, S., & Van Veen, B. (2007). *Signals and systems*. John Wiley & Sons.
- Henriquez, P., Alonso, J. B., Ferrer, M. A., & Travieso, C. M. (2014). Review of automatic fault diagnosis systems using audio and vibration signals. *IEEE Transactions on Systems, Man, and Cybernetics: Systems*, 44(5), 642-652.
- Henriquez, P., Alonso, J. B., Ferrer, M. A., & Travieso, C. M. (2014). Review of automatic fault diagnosis systems using audio and vibration signals. *IEEE Transactions on Systems, Man, and Cybernetics: Systems*, 44(5), 642-652.
- Hwang, W., Han, K., & Huh, K. (2012). Fault detection and diagnosis of the electromechanical brake based on observer and parity space. *International Journal of Automotive Technology*, 13(5), 845-851.
- Hwang, W., Han, K., Huh, K., Jung, J., & Kim, M. (2011, October). Model-based sensor fault detection algorithm design for Electro-Mechanical Brake. In *Intelligent Transportation Systems (ITSC), 2011 14th International IEEE Conference on* (pp. 962-967). IEEE.
- Jegadeeshwaran, R., & Sugumaran, V. (2015). Brake fault diagnosis using Clonal Selection Classification Algorithm (CSCA)—a statistical learning approach. *Engineering Science and Technology, an International Journal*, 18(1), 14-23.
- Jegadeeshwaran, R., & Sugumaran, V. (2015). Fault diagnosis of automobile hydraulic brake system using statistical features and support vector machines. *Mechanical Systems and Signal Processing*, 52, 436-446.
- Kumar, D., Tu, D., Zhu, N., Shah, R. A., Hou, D., & Zhang, H. (2017). The Free-Swimming Device Leakage Detection in Plastic Water-filled Pipes through Tuning the Wavelet Transform to the Underwater Acoustic Signals. *Water*, 9(10), 731.
- Lei, Y., He, Z., & Zi, Y. (2008). A new approach to intelligent fault diagnosis of rotating machinery. *Expert Systems with applications*, 35(4), 1593-1600.

- Liu, J., Li, Y. F., & Zio, E. (2017). A SVM framework for fault detection of the braking system in a high speed train. *Mechanical Systems and Signal Processing*, 87, 401-409.
- Lubis, M. Z., Pujiyati, S., Hestirianoto, T., & Wulandari, P. D. (2016). Dissipative Nonlinear Schrödinger Equations with Singular Data. *J Appl Computat Math*, 5(305), 2.
- Prabhakar, S., Mohanty, A. R., & Sekhar, A. S. (2002). Application of discrete wavelet transform for detection of ball bearing race faults. *Tribology International*, 35(12), 793-800.
- Rabiner, L. R., & Schafer, R. W. (2007). Introduction to digital speech processing. *Foundations and Trends® in Signal Processing*, 1(1-2), 1-194.
- Recognize Speech, <http://recognize-speech.com/feature-extraction/wavelet-based-features>
- Rhee, S. K., Tsang, P. H. S., & Wang, Y. S. (1989). Friction-induced noise and vibration of disc brakes. *Wear*, 133(1), 39-45.
- Schafer, R. W., & Rabiner, L. R. (1975). Digital representations of speech signals. *Proceedings of the IEEE*, 63(4), 662-677.
- Scheirer, E., & Slaney, M. (1997, April). Construction and evaluation of a robust multifeature speech/music discriminator. In *Acoustics, Speech, and Signal Processing, 1997. ICASSP-97., 1997 IEEE International Conference on* (Vol. 2, pp. 1331-1334). IEEE.
- Sounds in Time and Frequency Domain. In *Signal Processing and*
- Tan, L., & Jiang, J. (2013). *Digital signal processing: fundamentals and applications*. Academic Press.
- Umamathy, K., Krishnan, S., & Rao, R. K. (2007). Audio signal feature extraction and classification using local discriminant bases. *IEEE Transactions on Audio, Speech, and Language Processing*, 15(4), 1236-1246.
- Weeks, M. (2010). *Digital signal processing using MATLAB & wavelets*. Jones & Bartlett Learning.

Wu, J. D., & Liu, C. H. (2008). Investigation of engine fault diagnosis using discrete wavelet transform and neural network. *Expert Systems with Applications*, 35(3), 1200-1213.

Zhou, D., Ji, H., He, X., & Shang, J. (2017). Fault Detection and Isolation of the Brake Cylinder System for Electric Multiple Units. *IEEE Transactions on Control Systems Technology*.

